# Interplay of network structure and talent configuration on wealth dynamics

Jaeseok Hur,[1] Meesoon Ha,[2,*] and Hawoong Jeong[1,3,†]

[1] *Department of Physics, Korea Advanced Institute of Science and Technology, Daejeon 34141, Korea*
[2] *Department of Physics Education, Chosun University, Gwangju, 61452, Korea*
[3] *Center of Complex Systems, KAIST, Daejeon 34141, Korea*

The economic success of individuals is often determined by a combination of talent, luck, and assistance from others. We introduce a new agent-based model that simultaneously considers talent, luck, and social interaction. This model allows us to explore how network structure (how agents interact) and talent distribution among agents affect the dynamics of capital accumulation through analytical and numerical methods. We identify a phenomenon as "talent configuration effect", which refers to the influence of how talent is allocated to individuals (nodes) in the network. We analyze this effect through two key properties: talent assortativity (TA) and talent-degree correlation (TD). In particular, we focus on three economic indicators: growth rate ($n_{\rm rate}$), Gini coefficient (inequality: $n_{\rm Gini}$), and meritocratic fairness ($n_{LT}$). This investigation helps us understand the interplay between talent configuration and network structure on capital dynamics. We find that, in the short term, positive correlations exist between TA and TD for all three economic indicators. Furthermore, the dominant factor influencing capital dynamics depends on the network topology. In scale-free networks, TD has a stronger influence on the economic indices than TA. Conversely, in lattice-like networks, TA plays a more significant role. Our findings intuitively explain why highly talented agents are more likely to become central hubs in the network and why social connections tend to form between individuals with similar talent levels (socioeconomic homophily).

## I. INTRODUCTION

It is always questionable which of talent, luck, and innate environment, has greatest impact in an individual's success. Pluchino *et al.* [1] recently proposed the 'talent *versus* luck' (TvL) model (see Fig. 1) to quantitatively assess the impact of talent and luck on an individual's success. In the TvL model, the number of good and bad events represents the total amount of opportunities for either the positive or negative aspects of the environment. They showed that under the mediocre environment with the same number of good and bad events, an individual's talent is not strongly related to success, whereas under the good environment with more good events than bad events, high talent tends to guarantee more success. It implies the importance of the environment, in which an individual's talent can be fully realized. In addition to the total opportunities, the agents an individual interacts with can also play a crucial role in wealth dynamics, further emphasizing environmental effects. Barabási emphasized the importance of networks in the universal laws of success [2], and Zhou *et al.* [3] also presented a generative model for network growth, in which nature (fitness) and nurture (social advantage) effects act simultaneously.

In this paper, we propose a general framework for capital dynamics in agent-based networks. We introduce a new model incorporating talent, luck, and social interaction (TLS). In the TLS model, talent acts as a fitness factor, increasing average capital accumulation. Luck introduces random fluctuations in capital holdings, while social interaction directs captial transfers towards with more connections during inter-agent exchange. Consequently, we analytically demonstrate that the TLS model can reproduce the earlier results of the TvL model [1] and the Bouchaud-Mézard model (BM) model [4]. This is because the TvL model and the BM model correspond to the TLS model without social interactions and agent talent heterogeneity, respectively.

Unlike the BM model and its extensions [5–8], where capital dynamics soley depend on network structure, in the TLS model, we consider both network structure and the distribution of talent across the network (talent configuration). This allows us ti explore the impact of the talent configuration on interactions among heterogeneous agents for a given network. We analyze this effect through three key economic indicators: growth rate, Gini coefficient (inequality), and meritocratic fairness.

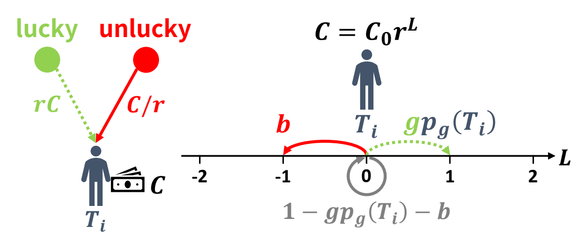


FIG. 1. Dynamics of talent *versus* luck (TvL) model. In the left panel, an agent $i$ with talent $T_i$ and capital $C$, meets either a lucky event with probability $g$ or an unlucky one with probability $b$. The lucky event gives chance to multiply capital by the factor $r > 1$, and the unlucky event always divides capital by $r$. In the right panel, the TvL model is illustrated as a one-dimensional random walk with probability $gp_g(T_i)$, $b$, and $1 - gp_g(T_i) - b$ to move from the original site in the capital level $L$ space to the right, to the left, and stay, where $L = m - n$ with the number of lucky (unlucky) events $m$ ($n$).

* msha@chosun.ac.kr
† hjeong@kaist.edu

We define two key properties to quantify talent configuration: talent assortativity (TA) and talent-degree correlation (TD). Our findings show a positive correlation between both TA and TD with all three metrics in the short term. Moreover, the dominant factor influencing these indices depends on the network topology. In scale-free networks, TD has a stronger impact compared to TD, whereas the opposite holds true for lattice-like networks. Finally, we intuitively explain why highly talented agents are more likely to become hubs and discuss the preferred form of socioeconomic homophily (similarity) in this context.

The remainder of this paper is organized as follows. In Sec. II, we propose the TLS model with the general framework of models for wealth dynamics, and explore the models by analytical because it is directly related to the TvL model and the BM model as its special cases and the corresponding mean-field version. In Sec. III. we define two talent configuration properties in the TLS model to speculate how they affect three economic indicators: growth rate, Gini coefficient, and meritocratic fairness. In Sec. IV, we conclude this paper as summarizing our findings with some remarks for further analytical needs as well as the discussion of possible future research topics.

## II. MODEL

Before moving onto the general analytic framework in the TLS model for wealth dynamics, we revisit the shortcoming of the TvL model and the BM model in the following subsections.

### A. Talent versus Luck (TvL) model

As illustrated in Fig. 1, the TvL model [1] is an agent-based model for the capital changes of $N$ individuals with the following parameters: $C(t) = \{C_1(t), \dots, C_N(t)\}$, which is the capital set of $N$ agents at time $t$. $T = \{T_1, \dots, T_N\}$, which is the talent set of $N$ agents. $\{g, b\}$ represent the probabilities of lucky and unlucky events, respectively, and $r$ the capital multiplier factor that is larger than 1.

The TvL model consists of $N$ agents with the discrete time $t$ $(t = 0, 1, \dots)$. Every agent starts with the initial capital $C_i(0) = C_0$. Agents' capitals can change, whereas talents are fixed over all the time. The talent distribution of agents follows a normal distribution, $T_i \sim \mathcal{N}(\mu, \sigma^2)$, where $\mu$ and $\sigma$ are the mean and the standard deviation of talent, respectively. It is important to note that $g+b \leq 1$, ensuring the total probability of events occurring remains within 0 and 1.

In Fig. 1, the probabilities of lucky, unlucky, and nothing happened events are $\{g, b, 1-g-b\}$, respectively. At each time $t$, one of three events occurs to every agent. For an arbitrary agent $i$, its capital changes one of the following three processes:

(i) When a lucky event occurs, a random number is generated from a uniform distribution between 0 and 1 (written as rand[0,1]). If it is smaller than the agent $i$'s talent $T_i$, its capital is increased by $r$ times, $C_i(t+1) = rC_i(t)$, if $\text{rand}[0,1] < T_i$. (ii) When an unlucky event occurs, its capital is reduced by $1/r$ times: $C_i(t+1) = C_i(t)/r$. (iii) When nothing happened event occurs, its capital remains the same as before, $C_i(t+1) = C_i(t)$.

Since $r$ is a constant, the amount of capital per agent is determined by the number of times that it wins and loses the capital by rules (i) and (ii). Let $m$ and $n$ represent the number of times the agent wins and loses capital according to rules (i) and (ii), respectively ($m = 0, 1, ...$, $n = 0, 1, ...$), so that the capital level $L \equiv m - n$. Then the amount of capital is equal to $C = C_0 r^L$. The probability that an agent $i$ gains the capital is equal to (the probability of lucky event occurring) $\times$ (the probability that rand[0,1] falls below $T_i$). To sum up, the probability of winning capital is $gp_g(T)$, where $p_g(T) = \min\{1, \max[T, 0]\}$, such that highly talented agents have more probability to seize their opportunities. The probability of an agent losing capital is simply equal to the probability of an unlucky event occurring $b$, and the probability of retaining capital is equal to $1 - gp_g(T) - b$.

The change of $L$ at each time step, $\Delta L$, can have a value among $\{-1, 0, 1\}$. However, the probability per each agent differs by the talent of agent. It can be considered as the ensemble of random walkers [9] as shown in Fig. 1. When talent $T$ is given, $\Delta L$ satisfies the following probability mass function:

$$p_L(\Delta L) = \begin{cases} b & \text{for } \Delta L = -1, \\ 1 - gp_g(T) - b & \text{for } \Delta L = 0, \\ gp_g(T) & \text{for } \Delta L = +1. \end{cases} \tag{1}$$

As the discrete time $t$ elapses, the probability that an agent with talent $T$ has a the capital level $L = m - n$, obeys the trinomial series as follows:

$$P_t(m, n) = a^m b^n [1 - a - b]^{t-m-n} \frac{t!}{m!n!(t-m-n)!}, \tag{2}$$

where $a = p_g(T)$. For this case, we consider the following four statistical quantities of $P_t(L = m - n)$ as a function of time $t$: mean ($\mu_L$), standard deviation ($\sigma_L$), skewness ($\mathcal{S}_L$), and kurtosis ($\mathcal{K}_L$):

$$\mu_L(t) = t(a - b), \tag{3}$$

$$\sigma_L(t) = \sqrt{t}\sqrt{(a + b) - (a - b)^2}, \tag{4}$$

$$\mathcal{S}_L(t) = \frac{(a - b)\left[2(a - b)^2 - 3(a + b) + 1\right]}{\sqrt{t}\left[(a + b) - (a - b)^2\right]^{3/2}}, \tag{5}$$

$$\mathcal{K}_L(t) = 3 + \frac{1}{t}\left[-6 + \frac{12ab + (a + b) - (a - b)^2}{[(a + b) - (a - b)^2]^2}\right]. \tag{6}$$

As $t \to \infty$, skewness $\mathcal{S}_L \sim t^{-1/2} \to 0$ and kurtosis

$\mathcal{K}_L - 3 \sim t^{-1} \to 0$, just as the normal distribution. This is quite trivial because the sum of $\Delta L = \{-1, 0, +1\}$ independently drawn from the same probability mass function follows the central limit theorem.

### B. Stochastic Differential Equation of TvL model

In the TvL model that is described as a trinomial series $P_t(L)$, $\mu_L \sim t$, $\sigma_L \sim t^{1/2}$, $\mathcal{S}_L \to 0$ and $\mathcal{K}_L \to 3$ as $t \to \infty$. Therefore, the motion of the capital level $L$ can be approximated by the Brownian motion and its drift $v_L(\equiv \mu_L/t)$ and volatility $\theta_L(\equiv \sigma_L/\sqrt{t})$ as a function of talent $T$, such that

$$v_L(T) = gp_g(T) - b, \tag{7}$$

$$\theta_L(T) = \sqrt{(gp_g(T) + b) - (gp_g(T) - b)^2}. \tag{8}$$

Then we can rewrite the model to stochastic differential equation (SDE) for the capital level $L$ per agent with talent $T$ as follows:

$$dL = v_L(T)dt + \theta_L(T)dW_t, \tag{9}$$

where $dt$ is the time interval, $W_t$ is Wiener process, $v_L$ is drift, and $\theta_L$ is volatility. To represent this equation for capital $C$, we assume that

$$dC = \alpha C dt + \beta C dW_t,$$

where the percentage drift $\alpha$ and the percentage volatility $\beta$ can be written by the drift $v_L$ and volatility $\theta_L$ by using the identity of $C$ and $L$ as well as Ito calculus, such that

$$\beta = \ln r \cdot \theta_L, \tag{10}$$

$$\alpha = \ln r \cdot v_L + \frac{1}{2}\beta^2. \tag{11}$$

Hence, the SDE of the TvL model can be written with parameters $(r, g, b, T)$ as follows:

$$dC = \alpha(T)C dt + \beta(T)C dW_t, \tag{12}$$

which is the well-known geometric Brownian motion (GBM). If the talent distribution follows the normal distribution, $T_i \sim \mathcal{N}(\mu, \sigma^2)$, Eq. (12) becomes

$$dC_i = \alpha(T_i)C_i dt + \beta(T_i)C_i dW_{t,i}, \tag{13}$$

where $C_i$ is the capital of an agent $i$, $T_i$ is the talent of an agent $i$, and $W_{t,i}$ is the Wiener process of $i$ at time $t$. It is noted that Wiener processes for all agents are independent and follow the Ito interpretation.

To determine this continuous SDE is in a good approximation for the TvL model, the numerical results of the discrete version should be compared with those of the continuous one. It can be said that the SDE is in a good approximation if the $L$ distributions are identical in both versions, see Supplemental Material (SM), Sec. I and Fig. S1 [10].

Lastly, we discuss the capital distribution and its power-law behavior in the TvL model. The capital distribution of the GBM does not show any power-law since it follows a log-normal distribution. Therefore, the capital distribution in the TvL model also follows the Gaussian sum of the log-normal distribution. However, the normalized capital $c \equiv C/\bar{C}$ distribution in both the GBM and the TvL model show the power-law behavior. The Fokker-Planck equation of the GBM with talent $T$ can be written as

$$\frac{\partial \rho}{\partial t} = \frac{1}{2}\frac{\partial^2}{\partial c^2}[\beta^2 c^2 \rho], \tag{14}$$

where the equilibrium condition is $\partial\rho/\partial t = 0$, so that Eq. (14) becomes the well-known Cauchy-Euler equation. Thus, the equilibrium solution of $c$ distribution for the GBM is

$$\rho_{eq}(c) = Ac^{-1} + Bc^{-2},$$

where we check two constants $A$ and $B$ by numerical. In the long-term regime, we observe that $\rho(c) \to \rho_{eq}(c)$ and $B = 0$, see SM, Sec.II and Fig.S2 [10]. Therefore, the GBM follows power-law as $\rho(c) \sim c^{-\gamma}$ with its power-law exponent $\gamma = 1$.

Based on Eq. (14), the capital distribution converges to $c^{-1}$, which is no longer as a function of $T$. Therefore, for all agents with the talent distribution $T_i \sim \mathcal{N}(\mu, \sigma^2)$ also follows $\rho_{eq}(c) \sim c^{-1}$ in the limit of $t \to \infty$. Since the Pareto distribution with $1 < \gamma < 2$ gives Gini coefficient (the index of the inequality) as 1, and both two models always converge to a global condensation state. It implies that a single agent monopolize almost the entire capital of the system as $t \to \infty$.

### C. Integrated model with Interaction

We propose a new model that consists of talent, luck, and social interaction (TLS) as introducing the terms of social interaction to the TvL model:

$$dC_i = \alpha(T_i)C_i dt + \beta(T_i)C_i dW_{t,i} + \sum_{j(\neq i)} (J_{ij}C_j - J_{ji}C_i)\, dt, \tag{15}$$

where the last interaction term was also suggested by Bouchaud and Mézard [4] to describes capital transfer by exchange between agent $i$ and agent $j$.

In this paper, we consider the matrix element $J_{ij}$ by introducing the pooling and sharing [11] interaction, so that every agent acts as both a sharing node and a pooling node, so that

$$J_{ij} = \begin{cases} J/k_j & \text{if } a_{ij} = 1, \\ 0 & \text{if } a_{ij} = 0, \end{cases} \tag{16}$$

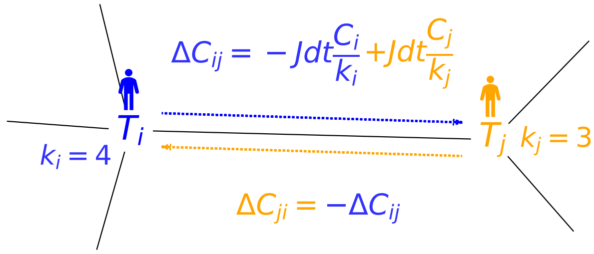


FIG. 2. Illustration of Pooling-sharing interaction [11]. The capital of $JdtC_i/k_i$ is given to all neighbors of agent $i$, and agent $j$ does in the same manner [12]. For this exchange between the link of $i$ and $j$, agent $i$ takes relatively more ratio of capital from agent $j$ because $k_i$ is larger than $k_j$.

where $a_{ij}$ is the element of adjacency matrix, either 1 or 0, $J$ is a constant as exchange strength, and $k_j$ is the degree of agent $j$, see Fig. 2. For the simplicity, let $\alpha(T_i) = \alpha_i$ and $\beta(T_i) = \beta_i$ then Eq. (15) with Eq. (16) becomes

$$dC_i = \alpha_i C_i dt + \beta_i C_i dW_{t,i} - Jdt \sum_{\{j|a_{ij}=1\}} \left( \frac{C_i}{k_i} - \frac{C_j}{k_j} \right). \tag{17}$$

As shown in Fig. 1 and Fig. 2, capital dynamics in the TLS model is influenced by individual talent, luck, and interaction among agents. First, all agents give $JdtC_i/k_i$ the amount of capital to its all connected neighboring agents, so that they send $JdtC_i$ to their neighbors with the same fraction of capital at each time step. In Eq. (17), the interaction term represents capital transfer between the connected link of agent $i$ and $j$, where agent $i$ gives $JdtC_i/k_i$ the amount of capital to $j$ and $j$ does vice versa. For the case of $C_i = C_j$, the agent who has larger degree $k$, gains more capital from the opponent by exchange. We call this kind of advantage as 'high-degree advantage'. Hence, in the TLS model, higher talent and higher degree are advantageous to capital growth. It can be regarded as individual advantage (or nature) and social advantage (or nurture) for each agent, in the context of the concept suggested by Zhou *et al.* [3].

In the TLS model, the network structure described by $a_{ij}$ also affects capital dynamics. For the complete network described by adjacency matrix $a_{ij} = 1 - \delta_{ij}$, where $\delta_{ij}$ is Kronecker delta, 1 if $i = j$ and 0 otherwise. For this case, the interaction term simply becomes as

$$-Jdt \left[ (\frac{N}{N-1})C_i - (\frac{N}{N-1})\bar{C} \right] \simeq -Jdt(C_i - \bar{C}),$$

where $N$ is large enough. The term of $-Jdt(C_i - \bar{C})$ is exactly the same as that in the mean-field BM model [4]. Therefore, the TLS model on a large complete network approximately is the same as the mean-field TLS model. Moreover, a sufficiently dense network gives similar capital dynamics, just like that in the mean-field TLS model.

### D. Mean-field TLS model

To discuss the analytic result of the mean-field TLS model, we need to revisit the GBM and and the mean-field BM model, in the context of the SDE as follows:

$$dC_i = \alpha C_i dt + \beta C_i dW_{t,i}, \tag{18}$$
$$dC_i = \alpha C_i dt + \beta C_i dW_{t,i} - Jdt(C_i - \bar{C}), \tag{19}$$

where $\alpha$ and $\beta$ are constants. The mean capital in both models are the same as $\langle C \rangle = C_0 e^{\alpha t}$. Summing up all equations in Eq. (19) over the agent index $i$, the interaction term is canceled out, and the ensemble average of $dC$ just follows the sum of the same GBM. In other words, the mean-field interaction does not change the mean capital, which is also the same as the GBM so far. As shown in Fig. 2, the interaction term takes the general form as follows:

$$\sum_{j(\neq i)} J_{ij} C_j - \sum_{j(\neq i)} J_{ji} C_i. \tag{20}$$

Using Eq. (20), we construct the SDE of the normalized capital in the mean-field BM model, so that:

$$dc = J(1-c)dt + \beta c dW_t. \tag{21}$$

The corresponding Fokker-Planck equation becomes

$$\frac{\partial \rho}{\partial t} = -\frac{\partial}{\partial c}\left[J(1-c)\rho\right] + \frac{1}{2}\frac{\partial^2}{\partial c^2}\left[(\beta c)^2 \rho\right]. \tag{22}$$

Then the equilibrium distribution of normalized capital $c$ that satisfies the condition of $\partial\rho/\partial t = 0$, is known as

$$\rho_{eq}(c) = \frac{(\frac{2J}{\beta^2})^{1+\frac{2J}{\beta^2}}}{\Gamma(1+\frac{2J}{\beta^2})} \cdot c^{-(2+\frac{2J}{\beta^2})} e^{-\frac{2J}{\beta^2 c}}, \tag{23}$$

where $\Gamma(x)$ is a Gamma function and $\rho_{eq}(c) \sim c^{-\gamma}$ with the power-law tail exponent of $\gamma = 2 + 2J/\beta^2$. It is noted that this result comes from $\langle C \rangle = C_0 e^{\alpha t}$.

Consider the relationship between the TvL model and the mean-field TLS model as follows:

$$dC_i = \alpha_i C_i dt + \beta_i C_i dW_{t,i}, \tag{24}$$
$$dC_i = \alpha_i C_i dt + \beta_i C_i dW_{t,i} - Jdt\left(C_i - \bar{C}\right), \tag{25}$$

where $\alpha_i = \alpha(T_i)$ and $\beta_i = \beta(T_i)$. For our case, the talent distribution follows the normal distribution, and the mean capital of the TvL model is the Gaussian sum of $e^{\alpha(T)t}$. In the short-term regime, this mean capital does not show exponential growth, see SM, Sec. II and Fig. S3 [10]. Summing all second equations over agent index $i$, the interaction term is still canceled out.

Nevertheless, the mean capital in the mean-field TLS model is not equal to that in the TvL model because the sum of $dC_i$ is the sum of different GBMs. Capital transfer by the mean-field interaction $-Jdt(C_i - \bar{C})$ makes relative changes in agent capitals, but it does not change the total capital at that time. However, this relative capital changes between talent-heterogeneous agents makes difference in capital growth eventually. This talent heterogeneity makes a system more complex.

In order to solve Eq. (25),

$$\langle C\rangle = C_0 e^{\tilde{\alpha}t}$$

is assumed, where $\tilde{\alpha}$ is constant. Then the SDE for the normalized capital $c_i$ with talent $T_i$ becomes

$$dc_i = [J - K_i c_i]dt + \beta_i c_i dW_{t,i}, \tag{26}$$

where $K_i = J + \tilde{\alpha} - \alpha_i$. The Fokker-Planck equation of Eq. (26) becomes

$$\frac{\partial \rho_i}{\partial t} = -\frac{\partial}{\partial c_i}\left[\{J - K_i c_i\}\rho_i\right] + \frac{1}{2}\frac{\partial^2}{\partial c_i^2}\left[(\beta_i c_i)^2 \rho_i\right]. \tag{27}$$

For the condition $\partial\rho_i/\partial t = 0$ in Eq. (27), the equilibrium solution of the normalized capital distribution $\rho_{eq,i}$ for the $T_i$ talented group is

$$\rho_{eq,i}(c_i) = \frac{\left(\frac{2J}{\beta_i^2}\right)^{1+\frac{2K_i}{\beta_i^2}}}{\Gamma(1+\frac{2K_i}{\beta_i^2})} \cdot c_i^{-(2+\frac{2K_i}{\beta_i^2})} e^{-\frac{2J}{\beta_i^2 c_i}}. \tag{28}$$

If $T_i \sim \mathcal{N}(\mu, \sigma^2)$ is considered, Eq. (28) can be integrated over all agents' $T_i$ as follows:

$$\rho_{eq}(c) = \int_{-\infty}^{\infty} \frac{e^{-\frac{(T-\mu)^2}{2\sigma^2}}}{\sigma\sqrt{2\pi}} \cdot \frac{\left(\frac{2J}{\beta^2}\right)^{1+\frac{2K}{\beta^2}}}{\Gamma(1+\frac{2K}{\beta^2})} \cdot c^{-(2+\frac{2K}{\beta^2})} e^{-\frac{2J}{\beta^2 c}} dT. \tag{29}$$

By the numerical simulation of the SDE for the mean-field TLS model, we check the assumption as well as the solution. To do so, we define $\alpha_{\rm ex}$ as follows:

$$\alpha_{\rm ex} = \frac{\ln\left(\langle C\rangle/C_0\right)}{t}. \tag{30}$$

If the mean capital of the system grows exponentially, $\alpha_{\rm ex}$ must be a constant. The time evolution of $\alpha_{\rm ex}$ is tested in SM, see Fig. S2 [10] (and insets in Fig. 4). Figure 3 shows the numerical results for the equilibrium normalized capital distribution of the mean-field TLS model for more information in SM, Fig. S4 [10].

As summarized in Table I, for the power-law behaviors on $\rho_{eq}(c)$ in mean-field models, the maximum and minimum of power-law tail exponent $\gamma$ in the mean-field BM model only depend on $\beta(T)$. Thus,

$$\gamma_{\rm max,BM} = 2 + 2J/\beta(0)^2 \text{ and } \gamma_{\rm min,BM} = 2 + 2J/\beta(1)^2,$$

where $T$ is constant. However, in the mean-field TLS model, it is complicated because talent $T$ is not a constant but a variable of the normal distribution. Since the power-law tail exponent $\gamma$ in the mean-field models is equal to $\gamma_{\rm min,BM}$ and $\gamma_{\rm max,BM}$ under the condition of $(\mu \geq 1, \sigma = 0)$ and $(\mu \leq 0, \sigma = 0)$, respectively.

However, under the condition of $(0 < \mu < 1, \sigma \neq 0)$, the situation is more complicated. For this case, talent heterogeneity '$\sigma$' can also influence the power-law tail exponent $\gamma$, whereas it is only depends on control parameter $2J/\beta^2$ in the mean-field BM model. We also empirically find that $\gamma = 2 + \langle\frac{2J}{\beta^2}\rangle - \delta$ under the condition

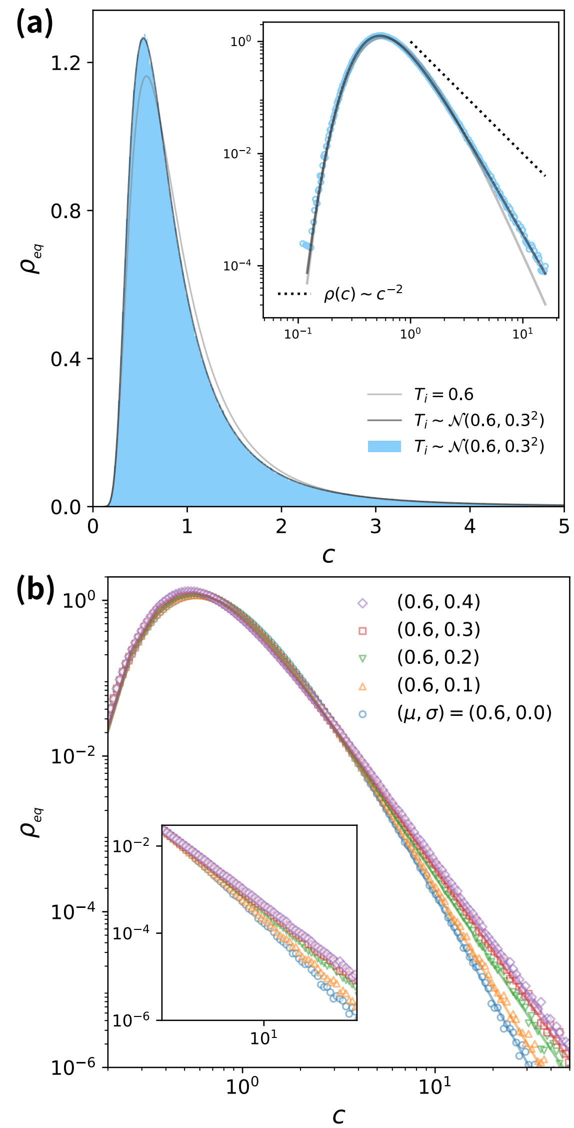


FIG. 3. Equilibrium normalized capital distribution in mean-field TLS model. (a) Colored area shows the result of normalized capital histogram as $t \to \infty$ for the condition of $(N, r, g, b, J) = (2\times10^6, 2, 0.1, 0.1, 0.1)$ and $(\mu, \sigma) = (0.6, 0.3)$. Gray and black solid lines are the analytic solutions of the mean-field BM model, Eq. (19) and the mean-field TLS model, Eq. (25), respectively. The inset shows the double-logarithmic scaled plots of the main plots. (b) For a variety of the standard deviation $\sigma$ values with the same $\mu$, the decaying behavior of $\rho_{eq}$ is double-logarithmically plotted against $c$ and the different portion near $c = 10^1$ is shown in the inset.

TABLE I. Main results of wealth dynamics models. Here $\alpha_i = \alpha(T_i)$, $\beta = \beta(T_i)$, and the talent $T$ satisfies the normal distribution as $p(T) = \frac{1}{\sigma\sqrt{2\pi}} e^{-\frac{(T-\mu)^2}{2\sigma^2}}$. It is noted that an adjusting constant $\delta$ satisfies $0 \leq \delta \leq \langle \frac{2J}{\beta^2} \rangle$, depending $p(T)$.

| Model | Growth | $\rho_{eq}(c)$ | $\gamma$ |
|---|---|---|---|
| GBM: $dC_i = \alpha C_i dt + \beta C_i dW_{t,i}$ | Exponential: $\langle C \rangle = C_0 e^{\alpha t}$ | $\sim c^{-1}$ | 1 |
| TvL model: $dC_i = \alpha_i C_i dt + \beta_i C_i dW_{t,i}$ | Non-exponential: $\langle C \rangle = \int_{-\infty}^{\infty} p(T) C_0 e^{\alpha(T)t} dT$ | $\sim c^{-1}$ | 1 |
| Mean-field BM model: $dC_i = \alpha C_i dt + \beta C_i dW_{t,i}$ $-Jdt(C_i - \bar{C})$ | Exponential: $\langle C \rangle = C_0 e^{\alpha t}$ | $f(c; 1 + \frac{2J}{\beta^2}, \frac{2J}{\beta^2})^{\dagger}$ | $2 + \frac{2J}{\beta^2}$ |
| Mean-field TLS model: $dC_i = \alpha_i C_i dt + \beta_i C_i dW_{t,i}$ $-Jdt(C_i - \bar{C})$ | Exponential: $\langle C \rangle = C_0 e^{\tilde{\alpha} t}$, $(\alpha(0) < \tilde{\alpha} < \alpha(1))$ | $\int_{-\infty}^{\infty} p(T) f(c; 1 + \frac{2K(T)}{\beta(T)^2}, \frac{2J}{\beta(T)^2}) dT$ | $2 + \langle \frac{2J}{\beta^2} \rangle - \delta$ |

$^{\dagger} f(c; A, B) \equiv \frac{B^A}{\Gamma(A)} c^{-(1+A)} e^{-B/c}$ denotes the inverse-Gamma distribution.

of $0 < \mu < 1$ and $\sigma \neq 0$, where $\langle \cdots \rangle$ means the ensemble average and $\delta$ is a adjusting constant. In particular, $\delta$ depends on the talent distribution in the system. For a given $\mu$, $\delta$ increases over $\sigma$ increases because high $\sigma$ gives a wide variance of $\alpha(T)$ that is corresponds to individual's average money making ability and intensify inequality, see Fig. 3.

Before moving onto Sec. III, we address a couple of interesting remarks among mean-field models: (i) The BM model without interaction is exactly the same as the GBM. The mean capital of both the BM model and the GBM are exponential. (ii) The TLS model without interaction is exactly the same as the TvL model. However,there is a big difference between two model. The mean of capital in the TvL model does not exponentially grows, whereas the mean capital in the mean-field TLS model does. This means that the mean-field interaction plays a different role in model details. In the BM model, the mean-field term does not change the dynamics regarding the mean capital, whereas in the TvL model, it does. Regarding power-law tail exponent $\gamma$, talent heterogeneity does not change $\gamma$ of non-interactive models but changes $\gamma$ for mean-field models. The characteristics of each wealth dynamics model is summarized in Table I.

## III. TALENT CONFIGURATION EFFECT

In order to analyze the effects of talent configuration properties on capital dynamics, we consider the TLS model on agent-based networks. In particular, we focus on three economic indices: the growth rate $n_{\text{rate}}$, the inequality $n_{\text{Gini}}$, the meritocratic fairness $n_{LT}$.

These three indices are defined as follows:

$$n_{\text{rate}} \equiv \frac{\langle C \rangle}{C_0}, \tag{31}$$

which is the index for the growth rate that represents how many times the system has grown, $n_{\text{rate}} \in [0, \infty]$.

$$n_{\text{Gini}} \equiv \frac{1}{2\langle C \rangle} \int_{-\infty}^{\infty} \int_{-\infty}^{\infty} p(C) p(C') |C - C'| dC dC', \tag{32}$$

which is the index for the inequality (Gini coefficient) that represents the inequality depicted by Lorenz curve, $n_{\text{Gini}} \in [0, 1]$. So $n_{\text{Gini}} = 0$ means system is perfectly equal and $n_{\text{Gini}} = 1$ means system is perfectly unequal.

$$n_{LT} \equiv \frac{\langle LT \rangle - \langle L \rangle \langle T \rangle}{\sqrt{Var(L) Var(T)}}, \tag{33}$$

which is the index for the meritocratic fairness that represents how much talent and following reward are related to each other, defined as Pearson correlation coefficient between the capital level $L = \log_r(C/C_0)$ and talent $T$, $n_{LT} \in [-1, 1]$. So $n_{LT} = -1$ means that $L$ and $T$ are perfectly anti-correlated (meritocratically unfair), $n_{LT} = 0$ means that there is no correlations between $L$ and $T$ (meritocratically neutral), and $n_{LT} = 1$ means that $L$ and $T$ are perfectly correlated (meritocratically fair).

In the TLS model, we also denote the following environmental parameters: capital multiplier $r$, lucky event probability $g$, unlucky event $b$, and exchange strength $J$. In addition, the network structure is described by the elements of an adjacency matrix $a_{ij}$. Since we consider that network links have no direction and weight, the adjacency matrix is symmetric and its elements $a_{ij}$ gives a value, either 0 or 1, and the matrix size is $N \times N$.

Describing talent configuration, we employ the talent distribution $p(T)$. For node index $i = 1, \ldots, N$, the talent configuration is defined as a vector $\mathbf{T} = (T_1, \ldots, T_N)$. There are the huge number of cases that allocate talent samples $(T_1, \ldots, T_N)$ to nodes for a given network. To obtain the numerical results in the TLS model, we need to set all the parameters for the environment $(r, g, b, J)$, the network structure $a_{ij}$, the talent distribution $p(T)$, and talent configuration vector $\mathbf{T} = (T_1, \ldots, T_N)$.

Estimating the effects of talent configuration on capital dynamics, we control the setting of parameters. Even though all parameters are all set, some network cases make talent configuration may be invalid to capital dynamics. If $a_{ij} = 0$, there are no links that are equal to the non-network case. For this case, Eq. (17) is the same as the TvL model, and talent configuration does not affect capital dynamics. If $a_{ij} = 1 - \delta_{ij}$, all agents have links to all other agents, so that talent configuration does not affect capital dynamics as well. While the non-network case have the mean degree $\bar{k}$ as 0, the complete-network case have mean degree $\bar{k}$ as $N-1$. Therefore, the network condition that talent configuration effects is valid in the given network, satisfies the following inequality: $0 < \bar{k} < N-1$. It is noted that sufficiently large $\bar{k}$ gives the mean-field TLS-like dynamics and already known about the characteristics of the mean-field TLS model. Therefore, we investigate an extreme sparse network cases of $\bar{k} = 2$ without loss of generality.

In this paper, we analyze two representative network cases, the Barabási-Albert (BA) network [13] with the degree heterogeneity and the scale-free property, and the Watts-Strogatz (WS) network [14] with the small rewiring probability $p_{\mathrm{re}} = 0.1$ as well as the small-world property. For the BA network generation, the linear preferential attachment is used with one additional link attachment per node. For that case, precisely, the mean degree $\bar{k}$ becomes $2(1 - 1/N)$, so that $\bar{k} \to 2$ for $N \gg 1$. For the WS network generation, $\bar{k} = 2$ and the rewiring probability $p_{\mathrm{re}} = 0.1$ are chosen. When $p_{\mathrm{re}} = 0$, the WS network is equal to a cycle network. When $p_{\mathrm{re}} = 1$, all links are randomly rewired to others. The chosen parameter $p_{\mathrm{re}} = 0.1$ is small enough to consider that the WS network generated by this parameter value is more close to a lattice-like network. It is noted that the parameter setting of the environment and the talent distribution are $(r, g, b, J) = (2.0, 0.1, 0.1, 0.1)$ and $T_i \sim \mathcal{N}(0.6, 0.1^2)$, respectively, in most numerical simulations.

### A. Heterogeneous Talent effects on Networks: Growth rate and Inequality

Before analyzing capital dynamics between different talent configurations, in this subsection, we investigate how different talent distributions, Dirac-delta distribution (fixed talent) and the normal distribution (Gaussian talent) give different behaviors to capital dynamics in the TLS model. To estimate the effects of the talent heterogeneity, we control the environment, network topology, and talent configurations.

In Fig. 4, we plot the time evolution of the growth rate and Gini coefficient as a function of time for the non-network case with the average degree $\bar{k} = 0$ (no interaction among agents), the complete network case with the average degree $\bar{k} = N-1$, and the very sparse random networks cases for the BA network and the WS network ($p_{\mathrm{re}} = 0.1$) with the average degree $\bar{k} = 2$, where we consider random talent configuration that has no correlation between agents' talents and other measures.

In the TLS model, the $\bar{k} = 0$ case with fixed talent corresponds to the GBM, and that with Gaussian talent corresponds to the TvL model. Similarly, the $\bar{k} = N - 1$ case with fixed talent corresponds to the mean-field BM model, and that with Gaussian talent corresponds to the mean-field TLS model.

In the top panel of Fig. 4, (a) and (b) show the time

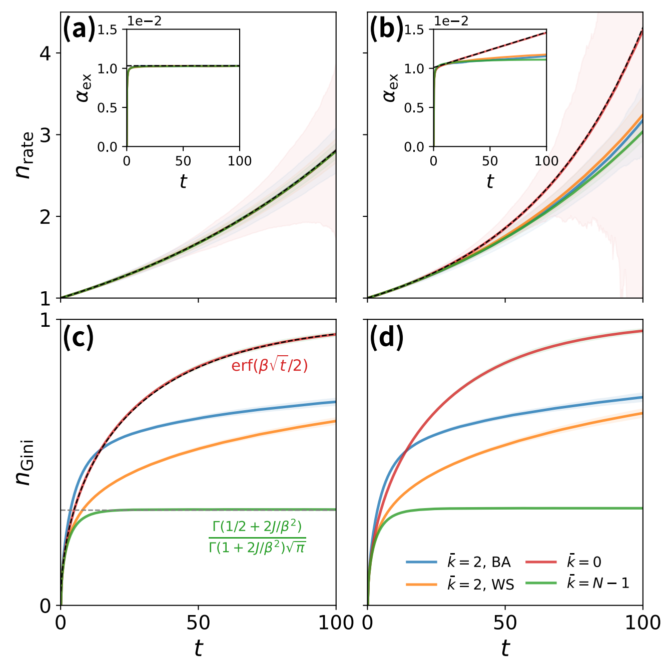


FIG. 4. Heterogeneous talent effect on growth rate, and Gini coefficient: $n_{\mathrm{rate}}$ for (a) and (b), and $n_{\mathrm{Gini}}$ for (c) and (d) against time $t$, where $\bar{k} = \{0, 2(\mathrm{BA}), 2(\mathrm{WS}), N-1\}$. Numerical results for a fixed talent $T_i = 0.6$ [(a) and (c), left] are compared with those for Gaussian talents $T_i \sim \mathcal{N}(0.6, 0.1^2)$ [(b) and (d), right]. We draw fitting lines by Eqs. (34) and (35) and also state the functional forms in (c). All simulation results are obtained for the same parameters $(N, r, g, b, J) = (10^4, 2, 0.1, 0.1, 0.1)$ and on the average of $2^{10}$ realizations, except for red solid lines with $2^{15}$ realizations. All colored regions show the standard deviation of realizations. Black dashed lines and gray dashed lines are the analytic solutions for $\bar{k} = 0$ and $\bar{k} = N-1$ cases, respectively. For (a) and (b), two insets show the time evolution of $\alpha_{\mathrm{ex}}$ denoted in Eq. (30). It is noted that for all cases, $r_{\mathrm{TA}} = 0$, $r_{\mathrm{TD}} = 0$, or they are not defined, see more details in Eq. (S2) and Eq. (37) of Sec. III B.

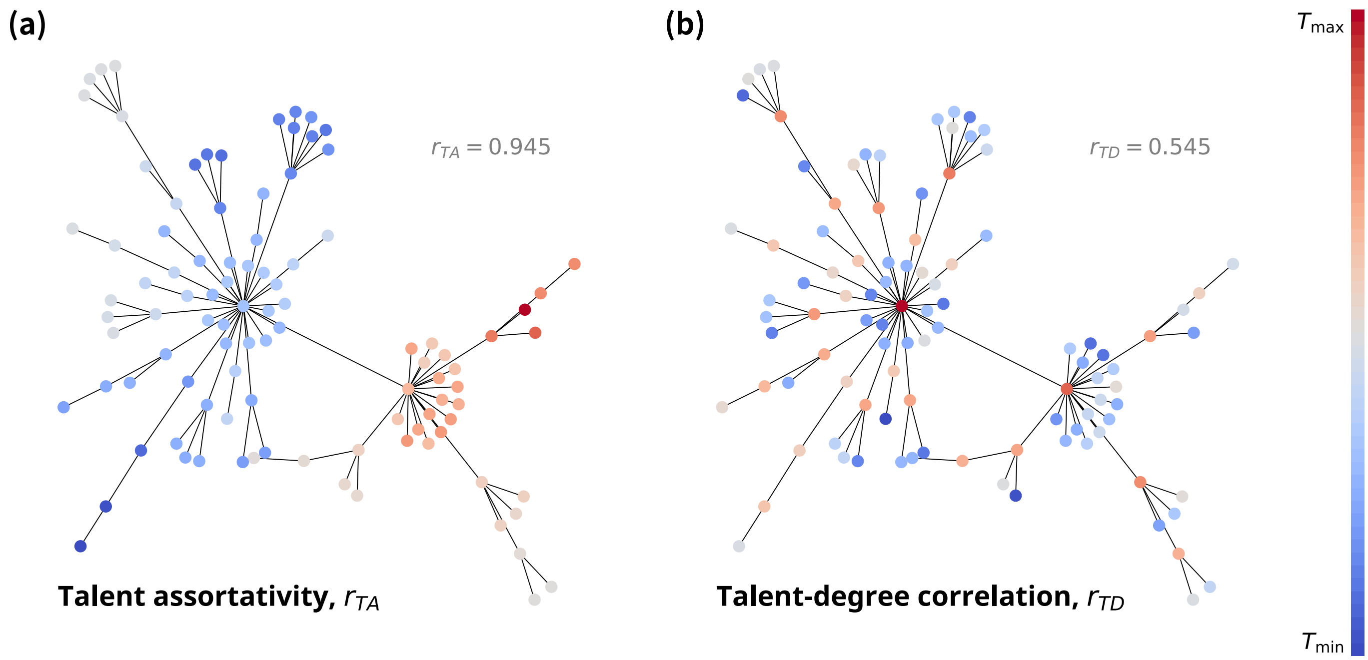


FIG. 5. Conceptual visualization for two talent configuration properties: (a) TA ($r_{\rm TA}$) and (b) TD ($r_{\rm TD}$). The sample network is the BA network with the number of agents $N = 100$ and the number of links $M = 99$. Nodal colors indicate high (red) or low (blue) talents, and talent samples follow the normal distribution $T \sim \mathcal{N}(\mu, \sigma^2)$. It is noted that $T_{\max}$ ($T_{\min}$) is the maximum (minimum) value for given talent samples. (a) shows an example for high TA case, where nodes with similar talents are clustered. (b) shows an example for high TD case, where highly talented nodes are allocated to hubs for a given network.

evolution of growth rate $n_{\rm rate}$, where all growth rate curves are the same for fixed talent but different only for Gaussian talent. This implies that the system growth does not depend on the network structure for fixed talent, whereas for Gaussian talent, it does. This result becomes a key difference between the BM model and the TLS model. We also argue the growth effective network structure or talent configuration in the TLS model, unlikely the BM model. Insets show the time evolution of $\alpha_{\rm ex}$, defined in Eq. (30). For fixed talent, all $\alpha_{\rm ex}$ values converge to the same value and grow exponentially, whereas for Gaussian talent, they become different and grow super-exponentially in short-time regime.

In the bottom panel of Fig. 4, (c) and (d) show the time evolution of the inequality $n_{\rm Gini}$, where they mainly depends on network structure but there are only slight differences between the fixed talent and Gaussian talent cases. The fixed talent cases with $\bar{k} = 0$ and $\bar{k} = N-1$ give as

$$n_{\rm Gini}(t) = {\rm erf}(\beta\sqrt{t}/2) \qquad \text{for } \bar{k} = 0, \tag{34}$$

$$\lim_{t\to\infty} n_{\rm Gini}(t) = \frac{\Gamma(1/2 + 2J/\beta^2)}{\Gamma(1 + 2J/\beta^2)\sqrt{\pi}} \qquad \text{for } \bar{k} = N-1, \tag{35}$$

which are the smallest and the largest mean degree gives the largest and the smallest of $n_{\rm Gini}$. In the short-term regime, the intermediate mean degree $\bar{k} = 2$, $n_{\rm Gini}$ depends on the network structure and the case of the BA network is slighter higher than that of $\bar{k} = 0$. This is consistent even for Gaussian talent cases.

### B. Talent Configuration (TC) properties: Talent Assortativity and Talent-Degree correlation

In this subsection, we quantify talent configuration properties on capital dynamics as two measures: 'talent assortativity' (TA), $r_{\rm TA}$, and 'talent-degree correlation' (TD), $r_{\rm TD}$.

By the link-based analysis, the TA property is denoted as

$$r_{\rm TA} \equiv \frac{Cov(T,T')}{\sqrt{Var(T)Var(T')}} = \frac{\sum_T \sum_{T'} TT'(e_{TT'} - q_T q_{T'})}{\sum_T T^2 q_T - (\sum_T T q_T)^2}. \tag{36}$$

The $r_{\rm TA}$ value is Pearson correlation coefficient for all links' talents $T$ and $T'$ for a given network, where $e_{TT'}$ is the probability that talent $T$ and $T'$ are connected in the network, $q_T$ is the probability that the nodes of randomly selected link have talent as $T$. By the node-based analysis, the TD property is denoted as

$$r_{\rm TD} \equiv \frac{Cov(T,k)}{\sqrt{Var(T)Var(k)}} = \frac{\langle Tk\rangle - \langle T\rangle\langle k\rangle}{\sqrt{Var(T)Var(k)}}. \tag{37}$$

The $r_{\rm TD}$ value is Pearson correlation coefficient for all nodes' talent $T$ and degree $k$.

A conceptual visualization for TA and TD properties are shown in Fig 5, where both $r_{\rm TA}$ and $r_{\rm TD}$ are increased as possible by pair swapping algorithms, see SM, pseudo-codes in Table S1 [10]. While $r_{\rm TA}$ reflects how many similar talents are connected for a given network, $r_{\rm TD}$ reflects how much higher talents have higher degrees for a given network. If the elements of the talent vector $\mathbf{T}$ are randomly permutated, these two talent configuration properties become 0.

For given a network and talent samples, we use a pair swapping algorithm to find a talent configuration $\mathbf{T}'$ that has a specific value of $r_{\rm TA}$ (or $r_{\rm TD}$) as we wish. The pair swapping algorithm for $r_{\rm TA}$ control consists of five steps:

1 Start with a graph $G$ and a talent vector $\mathbf{T}$.

2 Select a random pair of nodes for the graph $G$.

3 Let $\tilde{\mathbf{T}}$ be a talent vector, where selected two nodes are switched. For a target value $r'$, if $|r_{\rm TA}(G,\tilde{\mathbf{T}}) - r'| < |r_{\rm TA}(G,\mathbf{T}) - r'|$, accept $\tilde{\mathbf{T}}$ as a new $\mathbf{T}$.

4 Repeat 2 to 3 unless $|r_{\rm TA} - r'| < \epsilon$.

5 If $|r_{\rm TA} - r'| < \epsilon$, stop and print $\mathbf{T}$.

By the same algorithm, we also control $r_{\rm TD}$. However, this algorithm may not guarantee a target value $r'$. Although both $r_{\rm TA}$ and $r_{\rm TD}$ are defined as Pearson correlation coefficients and they lie in the interval [-1, 1], they do not mean that the minimum and maximum of $r_{\rm TA}$ and $r_{\rm TD}$ are -1 and 1, respectively.

Actual bounds for $r_{\rm TA}$ and $r_{\rm TD}$ depend on the detail of network structures. If we set a target value $r'$ to out of the real bound and set a error range $\epsilon$ to sufficiently a small value, the while loop in forth step 4 never stops. It is noted that the TA bounds were studied in [15]. Unlikely TA bounds, TD bounds are more easy to be controlled because they depend on the node-based analysis that does not influenced by the complex network topology. If all nodes have different degrees for a network, the minimum and maximum values of $r_{\rm TD}$ are exactly equal to -1 and 1, respectively, which are characterized by degree heterogeneity and were studied in [16].

For a given network, both $r_{\rm TA}$ and $r_{\rm TD}$ are measured. To test the pure $r_{\rm TA}$ ($r_{\rm TD}$) effect, one prefers to fix $r_{\rm TD}$ ($r_{\rm TA}$) as 0. However, both $r_{\rm TA}$ and $r_{\rm TD}$ are correlated under the single pair swapping. Therefore, we need to control two talent configuration properties at once in the random pair swapping algorithm. The pseudo-codes of algorithms for the dual value control are also summarized in SM as Table S1 [10] with some illustrations. The core argument of estimating a single talent configuration property is that the other one is in the sufficiently small error range of $\epsilon$, we consider this pair of ($r_{\rm TA}$, $r_{\rm TD}$) gives the quasi-pure effect of $r_{\rm TA}$ (or $r_{\rm TD}$). Throughout this procedure, we estimate the quasi-pure effect of $r_{\rm TA}$ (or $r_{\rm TD}$) on capital dynamics in the TLS model.

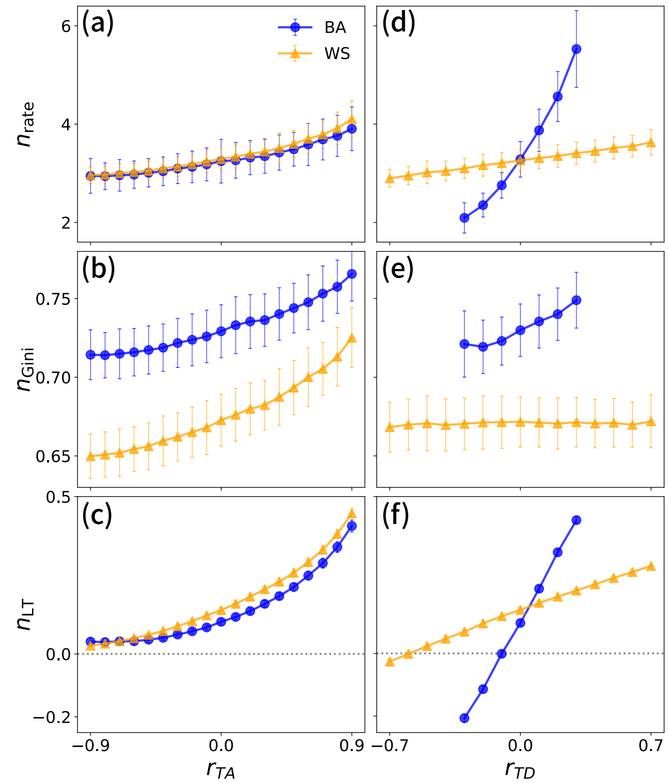


FIG. 6. TC effects on three economic indices in BA and WS networks: $n_{\rm rate}$, $n_{\rm Gini}$, and $n_{LT}$ against $r_{\rm TA}$ for (a)-(c), and $r_{\rm TD}$ for (d)-(f). In all simulations, the parameters are $(N, r, g, b, J) = (10^4, 2, 0.1, 0.1, 0.1)$ and $T_i$ has $(\mu, \sigma) = (0.6, 0.1)$. Dots (bars) show the average values of numerical results (standard deviation) at time $t = 100$ with $2^{10}$ realizations. The BA network is generated by one additional link attachment per node, and the WS network is generated with the rewiring probability $p_{\rm re} = 0.1$. Here both networks have the same mean degree $\bar{k} = 2$.

### C. Short-term Behaviors of TC effects

In this subsection, we present how to investigate effect of talent configuration (TC) properties, ($r_{\rm TA}$, $r_{\rm TD}$) on capital dynamics of the TLS model in BA and WA networks for the short-time scales $t \in [0, 100]$.

Figure 6 shows TC effects on BA and WS networks as a function of $r_{\rm TA}$ and $r_{\rm TD}$, respectively, which are obtained in short-term regime. It is noted that we collect TC for the quasi-pure $r_{\rm TA}$ and $r_{\rm TD}$ cases within the error range of $\epsilon = 10^{-2}$. The collected pairs of ($r_{\rm TA}$, $r_{\rm TD}$) are presented in SM, Sec. IV, and Fig. S5 [10]. All numerical data of $n_{\rm rate}$, $n_{\rm Gini}$, and $n_{LT}$ are measured at $t = 100$. All time evolutions for all three economic indices in BA and WS networks with the quasi-pure samples of $r_{TA}$ and $r_{TD}$ are shown in SM. Fig. S6 and S7 [10].

Based on the results in Fig. 6, we address the following three remarks: (i) Almost all indices have positive correlation with $r_{\rm TA}$ and $r_{\rm TD}$, except for (d), $r_{\rm TD}$ vs. $n_{\rm Gini}$ in the WS network. (ii) $n_{LT}$ cannot be negative for the

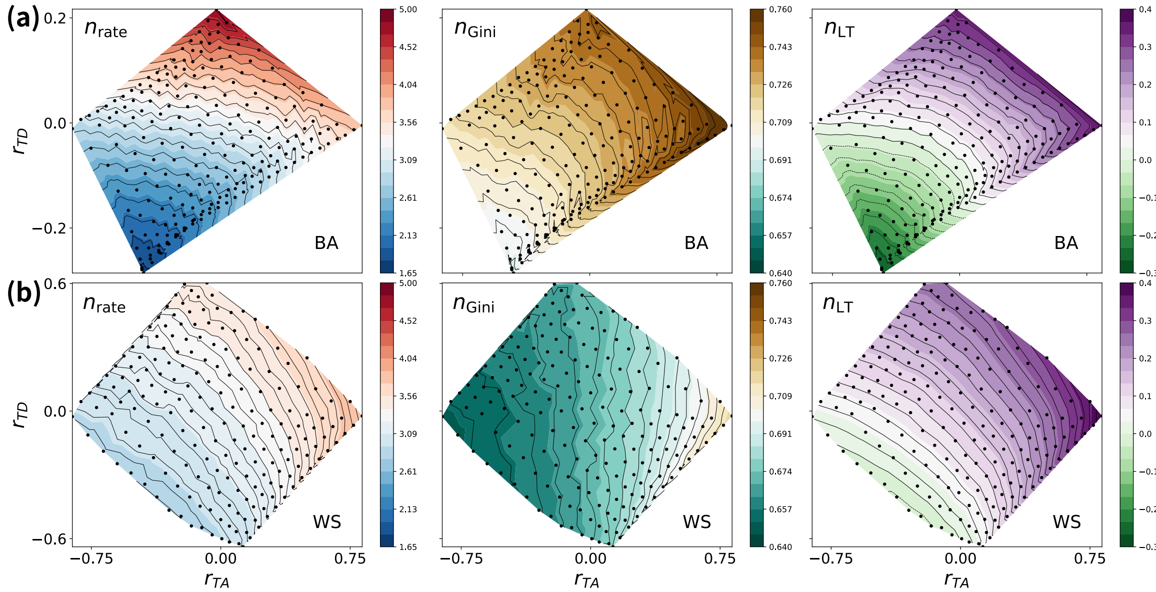


FIG. 7. Impact of TC properties on three economic indices. All simulations are performed for $(N, r, g, b, J) = (10^4, 2, 0.1, 0.1, 0.1)$ and $(\mu, \sigma) = (0.6, 0.1)$. Dots show the ordered pairs of $(r_{\rm TA},\ r_{\rm TD})$ and colored regions show the expected average values of indices at $t = 100$ with $2^7$ realizations. For (a), the BA network is generated by one additional link attachment per node, and for (b), the WS network is generated with the rewiring probability $p_{\rm re} = 0.1$. Here both networks have the same mean degree $\bar{k} = 2$.

quasi-pure $r_{\rm TA}$ case ($r_{\rm TD} \sim 0$), while it can for the quasi-pure $r_{\rm TD}$ case ($r_{\rm TA} \sim 0$). (iii) For the BA network, $n_{\rm rate}$ explosively increases as $r_{\rm TD}$ increases. In particular, the realization error only depends on $r_{\rm TD}$ for $n_{\rm rate}$. The first remark (i) shows the fact that both $r_{\rm TA}$ and $r_{\rm TD}$ are valid as an criterion for improving three economic indices $n_{\rm rate}$, $n_{\rm Gini}$, and $n_{LT}$. Meanwhile, it can be considered as the trade-off relation between "growth or meritocracy" and "equality", which matches to the common sense of economy. The remark (ii) shows that the less talent cannot get the more capital by the $r_{\rm TA}$ effect in the TLS model if there is no correlation between talent and degree for the given network. The remark (iii) shows that $r_{\rm TD}$ effect is critical to the degree-heterogeneous network, such as the BA network with the scale-free property. The 'high degree advantage' combined with high $r_{\rm TD}$ makes choice and concentration to highly talented agent, which yields an explosive growth in the system. As a result, the performance of the system depends on few agents but the system volatility increases. This is why highly talented agents are more likely to hubs and why economic systems are vulnerable to hub attacks (even more, higher talent gives higher percentage volatility $\beta$).

One can also consider the simultaneous effects of both $r_{\rm TA}$ and $r_{\rm TD}$. As shown in Fig. 7, the contour plots represent both $r_{\rm TA}$ and $r_{\rm TD}$ effects on (a) BA and (b) WS networks. Most indices have positive correlation between $r_{\rm TA}$ and $r_{\rm TD}$. In the BA network, $n_{\rm rate}$ is more sensitive to $r_{\rm TD}$ than $r_{\rm TA}$ since contour lines almost lie horizontally (along $r_{\rm TA}$-axis), and $n_{\rm Gini}$ is more sensitive to $r_{\rm TA}$ than $r_{\rm TD}$ since contour lines almost lie vertically (along $r_{\rm TD}$-axis). In the WS network with small rewiring probability, $p_{\rm re} = 0.1$ [17], all three indices $n_{\rm rate}$, $n_{\rm g}$, and $n_{LT}$ are more sensitive to $r_{\rm TA}$ than $r_{\rm TD}$.

## IV. SUMMARY AND DISCUSSION

We have proposed an agent-based model for capital dynamics with talent, luck and social interaction (TLS), named the TLS model, where we explored the model by analytical and numerical. In particular, we showed that the TLS model can be considered as the generalized framework to cover both the 'talent *versus* luck' (TvL) model and the Bouchaud-Mezárd (BM) model in context of the stochastic differential equation form. Inserting talent heterogeneity and interaction on agent-based networks to our model simultaneously, talent configuration (TC) plays a key role in capital dynamics, which was not considered in the BM model. Moreover, we found that the TC effect is only valid for $0 < \bar{k} < N - 1$. To estimate TC effects systematically, we employed three economic indices: $n_{\rm rate}$ (growth rate), $n_{\rm Gini}$ (inequality), and $n_{LT}$ (meritocratic fairness) to extract TC properties as talent assortativity (TA, $r_{\rm TA}$), and talent-degree correlation (TD, $r_{\rm TD}$).

Our study reveals that TA and TD are positively correlated in three economic indices. In addition, the dominant TC property depends on the network structure. Existing TvL research suggests that talent requires a supportive environment for full utilization. The environment refers to the total opportunity shared by all agents. We also introduced another environmental factor: the influence of neighboring agents. Unlike the aggregate opportunity, which is a global factor, network interactions are local. An agent's success is significantly influenced by its position within the network and the composition of its neighbors. Network locality restricts the benefits of interaction, and $r_{\rm TA}$ and $r_{\rm TD}$ determine who benefits most.

More precisely, high $r_{\rm TA}$ ensures that qualitative benefits (high-talent neighbors) are monopolized by high-talent clusters as high $r_{\rm TD}$ ensures that quantitative benefits (many neighbors and high order benefits) are monopolized by high-talent agents. While growth rates, inequality, and meritocratic fairness increase, high $r_{\rm TA}$ and high $r_{\rm TD}$ can initiate kind of cartel effect and centralization effect, respectively. In particular, selective interaction by high-talent clusters under the limited opportunity aggregate condition with even not so large probability for lucky events can promote the formation of a meritocratic society, see SM, Fig. S8 [10]. Our findings offer insights into socioeconomic homophily (clustering by similar socioeconomic characteristics) and resource concentration among elites. Conversely, socioeconomic integration appears crucial for reducing inequality.

For future studies, it would be interesting to quantify the long-term impact of talent configuration on the Gini coefficient (beyond our short-term analysis, $t \in [0, 100]$ [18]). Additionally, generalizing the TC effect to scale-free networks with various degree decay exponents and exploring its interplay with the shortcut effect in WS networks for different $p_{\rm re}$ and $\bar{k}$ values are promising avenues. Our model's limitations lie in the static nature of interactions, which currently do not affect total capital. Future extensions could incorporate (i) synergetic interactions that increase total capital and (ii) competitive interactions that favor highly talented agents in capital transfer. Alternatively, considering time-dependent talent changes could model agent productivity improvements. For zero-sum capital scenarios, individual growth depends on interaction-based transfers, similar to the yard-sale (YS) model [19, 20]. The YS model highlights the role of initial capital stock in such fixed-sum scenarios, further emphasized by Boghosian *et al.* [21] findings on discontinuous Gini coefficient variation under 'wealth attained advantage'. Finally, Lee and Lee's [22] work on generalized YS models on networks suggests exploring potential phase transitions and scaling behaviors in capital dynamics. Investigating the phase diagram of capital dynamics and condensation transitions could be another fruitful direction.

## ACKNOWLEDGMENTS

This research was supported by the Basic Science Research Program through the National Research Foundation of Korea (NRF) (KR) [Grant No. NRF-2020R1A2C1007703 (J.H., M.H.) and No. NRF-2022R1A2B5B02001752 (J.H., H.J.)].

---


[1] A. Pluchino, A. E. Biondo, and A. Rapisarda, Advances in Complex systems **21**, 1850014 (2018).

[2] A.-L. Barabási, *The formula: The universal laws of success* (Hachette UK, 2018).

[3] B. Zhou, P. Holme, Z. Gong, C. Zhan, Y. Huang, X. Lu, and X. Meng, Nature Communications **14**, 7031 (2023).

[4] J.-P. Bouchaud and M. Mézard, Physica A: Statistical Mechanics and its Applications **282**, 536 (2000).

[5] W. Souma, Y. Fujiwara, and H. Aoyama, arXiv preprint cond-mat/0108482 (2001).

[6] W. Souma, Y. Fujiwara, and H. Aoyama, in *Meeting the Challenge of Social Problems via Agent-Based Simulation: Post-Proceedings of the Second International Workshop on Agent-Based Approaches in Economic and Social Complex Systems* (Springer, 2003) pp. 37–49.

[7] D. Garlaschelli and M. I. Loffredo, Physica A: Statistical Mechanics and its Applications **338**, 113 (2004).

[8] D. Garlaschelli and M. I. Loffredo, Journal of Physics A: Mathematical and Theoretical **41**, 224018 (2008).

[9] R. Simão, F. Rosendo, and L. Wardil, Advances in Complex Systems **24**, 2150010 (2021).

[10] See Supplemental Material at [URL will be inserted by publisher] for more details, which includes Refs [1, 13–15, 23].

[11] V. Stojkoski, Z. Utkovski, L. Basnarkov, and L. Kocarev, Physical Review E **99**, 062312 (2019).

[12] The agent itself plays a role of pooling and sharing node in the system.

[13] A.-L. Barabási and R. Albert, Science **286**, 509 (1999).

[14] D. J. Watts and S. H. Strogatz, Nature **393**, 440 (1998).

[15] M. Cinelli, L. Peel, A. Iovanella, and J.-C. Delvenne, Physical Review E **102**, 062310 (2020).

[16] R. Jacob, K. Harikrishnan, R. Misra, and G. Ambika, Royal Society open science **4**, 160757 (2017).

[17] For sufficiently small rewiring probability $p_{\rm re} = 0.1$ makes the WS network have more lattice-like property like cycle network.

[18] Some preliminary results have been tested as our future study. As shown in SM, Fig. S8 (c) [10], $n_{\rm Gini}$ converges to 1 after long time later, regardless of $r_{TA}$ value when the network is very sparse as $\bar{k} = 2$. It seems to TA effects only play a role of delaying global wealth condensation. However, one may consider that the final destination of system inequality can differ for $r_{\rm TA}$ values in sufficiently dense networks.

[19] A. Chakraborti and B. K. Chakrabarti, The European Physical Journal B-Condensed Matter and Complex Systems **17**, 167 (2000).

[20] B. Hayes, American Scientist **90**, 400 (2002).

[21] B. M. Boghosian, A. Devitt-Lee, M. Johnson, J. Li, J. A. Marcq, and H. Wang, Physica A: Statistical Mechanics and its Applications **476**, 15 (2017).

[22] H. G. Lee and D.-S. Lee, Physical Review E **108**, 064303 (2023).

[23] V. Pareto, *Manual of political economy: a critical and variorum edition* (OUP Oxford, 2014).

# SUPPLEMENTAL MATERIAL FOR "INTERPLAY OF NETWORK STRUCTURE AND TALENT CONFIGURATION ON WEALTH DYNAMICS"

## S1. CORRESPONDENCE CHECK BETWEEN DISCRETE AND CONTINUOUS MODELS

This is the justification of capital dynamics in the talent versus luck (TvL) model between discrete and a continuous versions. In earlier simulation results by Pluchino, *et al.* [1], the rate of highly talented agents (talent is higher than $\mu + \sigma$) improved from its first condition ($C_0$) after 80 time step was about to 32 %. It is also written as $P_T = P(C_i > C_0 | T_i > \mu + \sigma)$. To mimic these results, in accordance with our numerical simulation, we employ the simple environmental parameter set as $(r, g, b) = (2, 0.1, 0.1)$. Under this condition, discrete and continuous versions give $P_{T,dis} = 0.253$ and $P_{T,con} = 0.294$, respectively, similar as $\sim 32$ % by using $(N, \mu, \sigma) = (10^6, 0.6, 0.1)$.

Since capital $C$ and capital level $L$ satisfy the identity $C = C_0 r^L \longleftrightarrow L = \log_r(C/C_0)$, we can say that the continuous TvL equation is in good approximation for the discrete TvL model under the condition that both discrete and continuous simulation results give the same capital level $L$ distributions. The $L$ distribution in the TvL model is the Gaussian sum of $L$ distributions of $T$ talented agent groups. If the $L$ distribution in discrete and continuous versions are the same for $T$ talented group, the whole distribution of Gaussian talented group would be the same. Figure S1 (a) shows the four statistics of discrete TvL and continuous TvL simulation results. The statistics of discrete model follows the theoretical prediction (gray line) as we mentioned in main text, see Eq. (3)–(6). The mean and standard deviation of two are slightly different since $dt$ is finite but almost same. However, the skewness and the kurtosis of the discrete model more slowly than those in the continuous model. Nevertheless, those two value converge to 0 and 3 as $t \to \infty$, just as the normal distribution. The $L$ distributions of two are almost the same as shown in Fig. **??** (b). According to this result, we can consider only the continuous TvL model from now on for the remainders.

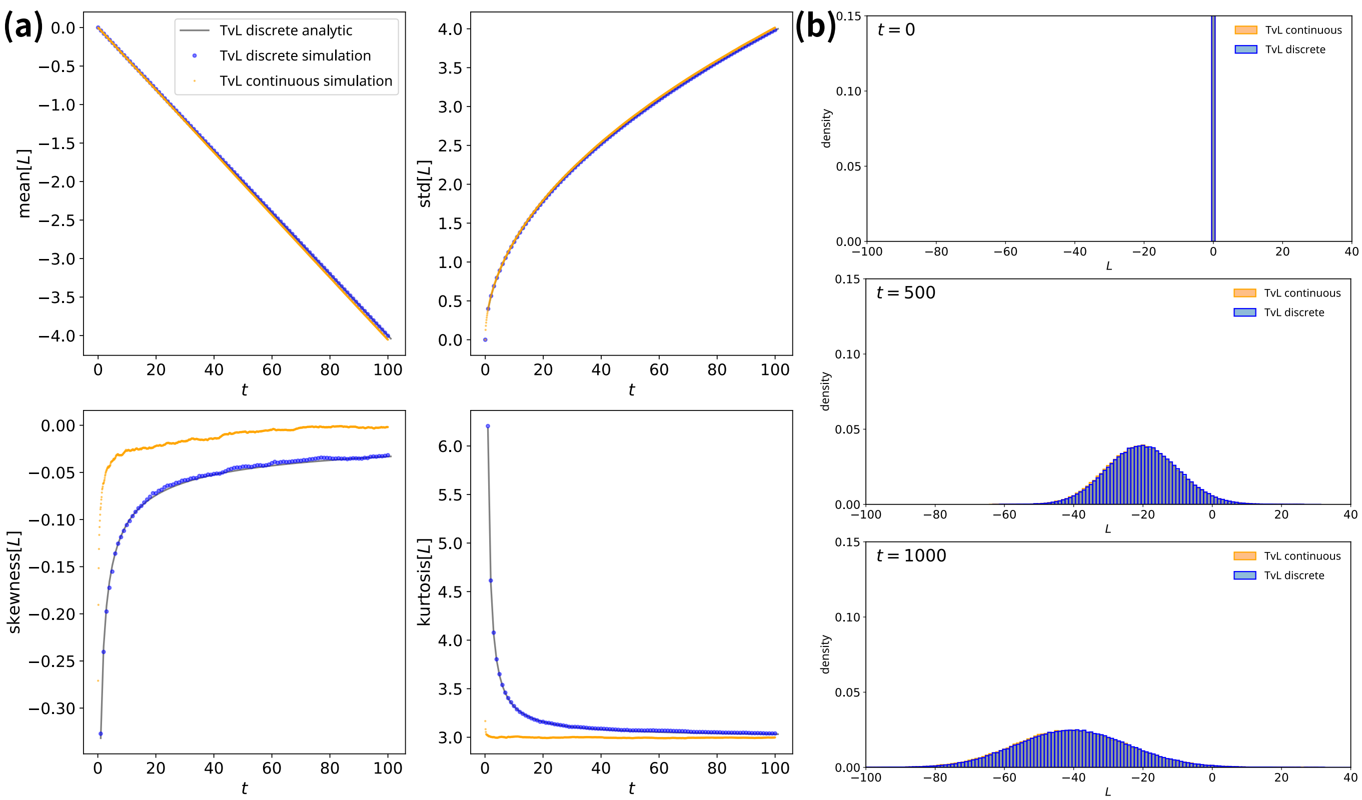


FIG. S1. Correspondence check of the TvL model between discrete and continuous versions. The discrete version is numerically simulated by capital change rules, see Fig. 1 in the main text, and the continuous version is numerically obtained by Eq. (13) in the main text. (a) Four statistics for the parameter set $(N, C_0, r, g, b, \mu, \sigma) = (10^6, 1, 2, 0.1, 0.1, 0.6, 0)$ and (b) histograms are shown in discrete and continuous versions of the TvL model for the parameter set $(N, r, g, b, \mu, \sigma) = (10^6, 2, 0.1, 0.1, 0.6, 0.1)$. Here the time increment $dt = 0.1$ is used for both versions.

## S2. ADDITION INFORMATION

### A. Power-law behavior in GBM and TvL model

We here mention that the equilibrium normalized capital distribution in the TvL model follows $\rho_{eq}(c) = Ac^{-1} + Bc^{-2}$, where $A$ and $B$ are constants, which is as a solution of the Fokker-Planck equation. Figure S2 shows that simulation results guarantees $B = 0$: (a) for both cases of $T_i = 0.6$ that is the same as the GBM, and (b) for $T_i \sim \mathcal{N}(0.6, 0.1^2)$ that is the same as the TvL model. These two distribution are the same as $\rho_{eq}(c) \sim c^{-\gamma}$ with $\gamma = 1$. This means that talent heterogeneity does not affect the equilibrium normalized capital distribution in the TvL model.

### B. Non-exponential growth of TvL model

The growth rate $\langle C\rangle/C_0$ in the TvL model as a function of $(r, g, b, \mu, \sigma)$ is given as follows:

$$\begin{aligned}\frac{\langle C\rangle}{C_0} =& \frac{1}{2\sqrt{2\sigma^2 Xt+1}} e^{\frac{-\mu^2 Xt+\mu Yt+\sigma^2 Y^2 t^2/2}{2\sigma^2 Xt+1} - Zt}\left[\mathrm{erf}\left(\frac{\mu+\sigma^2 Yt}{\sigma\sqrt{4\sigma^2 Xt+2}}\right) - \mathrm{erf}\left(\frac{\mu+\sigma^2(Y-2X)t-1}{\sigma\sqrt{4\sigma^2 Xt+2}}\right)\right] \\ &+ \frac{1}{2}e^{(-X+Y-Z)t}\left[1+\mathrm{erf}\left(\frac{\mu-1}{\sigma\sqrt{2}}\right)\right] + \frac{1}{2}e^{-Zt}\left[1-\mathrm{erf}\left(\frac{\mu}{\sigma\sqrt{2}}\right)\right], \end{aligned} \tag{S1}$$

where

$$X = \frac{g^2(\ln r)^2}{2},\ Y = g\ln r\left(1+\frac{\ln r}{2}+b\ln r\right),\ \text{and } Z = b\ln r\left(1-\frac{\ln r}{2}+\frac{b\ln r}{2}\right)$$

As shown in Fig. S3 (a), the simulation result fits the analytic solution very well. The inset shows $\alpha_{\rm ex} = \ln(\langle C\rangle/C_0)/t$ linearly increases as time $t$ elapses. It means the super-exponential growth. However, as $t \to \infty$, it converges to the some value. This converging value is related to the maximum value of $\alpha(r, g, b, T) = \ln r(gp_g(T) - b) + \frac{(\ln r)^2}{2}[(gp_g(T) + b) - (gp_g(T) - b)^2]$. Under the simulation condition of $(r, g, b) = (2, 0.1, 0.1)$, $T = 1$ gives the maximum and its value is $\alpha(2, 0.1, 0.1, 1) = 0.04805$, see Fig. S3 (b) as well.

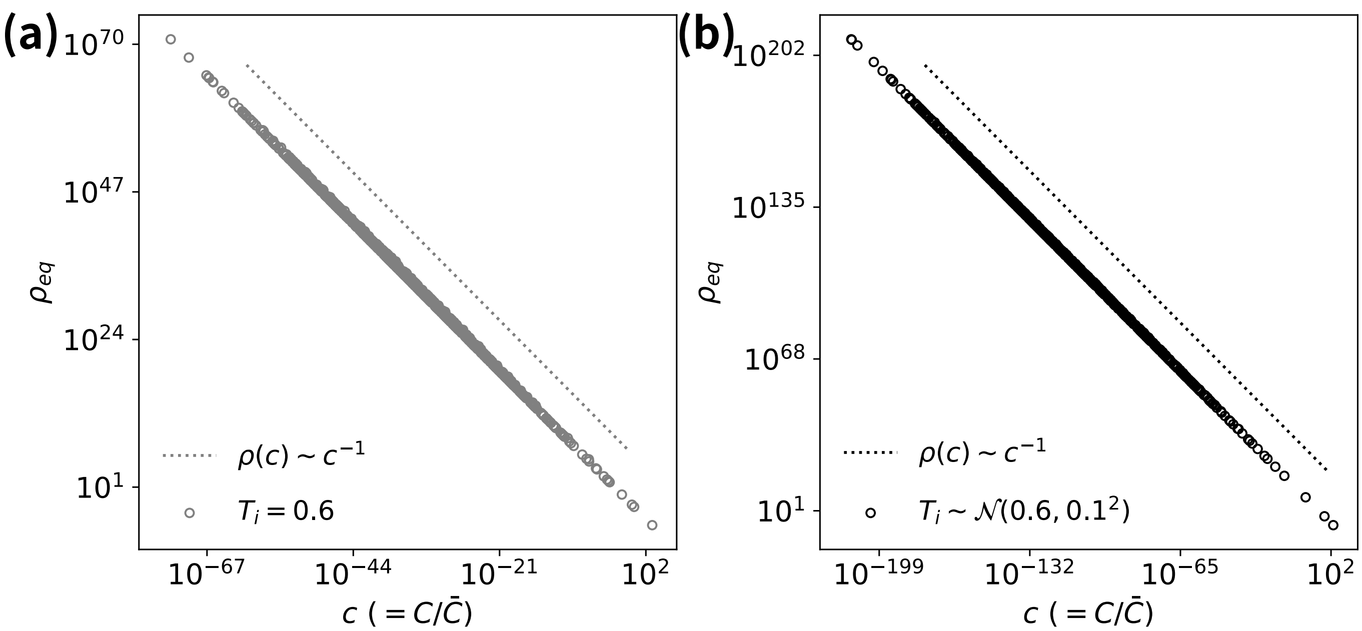


FIG. S2. Double-logarithmic scaled plots for equilibrium normalized capital distribution: (a) GBM and (b) the TvL model, where $T_i = 0.6$ for (a) and $T_i \sim \mathcal{N}(0.6, 0.1^2)$ for (b). Here the parameter set $(r, g, b) = (2, 0.1, 0.1)$ is used in numerical simulations.

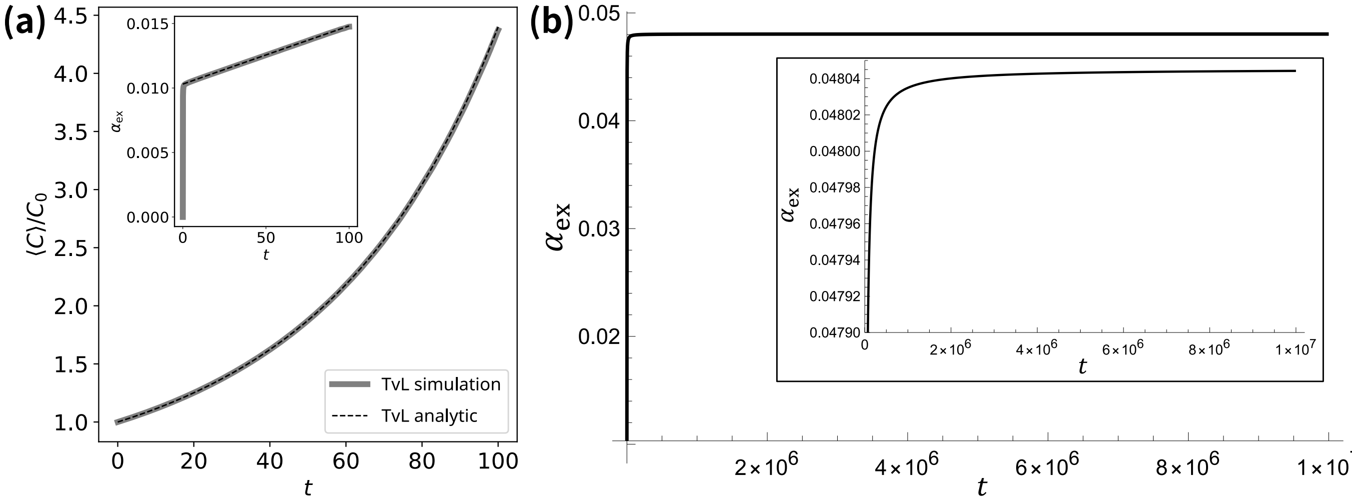


FIG. S3. Non-exponential growth rate $\langle C\rangle/C_0$ in TvL model. (a) The time evolution of $\langle C\rangle/C_0$ in the TvL model for $(N, r, g, b, \mu, \sigma) = (2^{10} \times 10^6, 2, 0.1, 0.1, 0.6, 0.1)$ with $dt = 0.1$. (b) The time evolution $\alpha_{\rm ex}$ in the TvL model for $(r, g, b, \mu, \sigma) = (2, 0.1, 0.1, 0.6, 0.1)$. The TvL motion super-exponentially starts, but eventually converges to the exponential growth with $\alpha_{\rm ex} \simeq \alpha(1) = 0.04805$.

### C. Mean-field TLS model

We here provide the addition information for the mean-field TLS model. For $(r, g, b) = (2, 0.1, 0.1)$, $\alpha(2, 0.1, 0.1, \mu = 0.6) = 0.0103$ but $\beta(2, 0.1, 0.1, \mu = 0.6) = 0.276$. It roughly means that the capital of average talented agent mainly depends on luck than talent 27 times more. The total capital grows exponentially because the mean capital of $T$ talented group is $C_0 e^{\alpha(T)t}$, but microscopically, the rate of agents that loses capital than initial state increases over time.

Figure S4 (a) shows the $L$ distribution for various models after 100 unit times. If $L = \log_r(C/C_0)$ is larger than 0, it means the capital is larger than the initial capital. The improvement rate $P_I = P(C > C_0)$ in the TvL model and the mean-field TLS model after 100 unit times are 0.16 and 0.97, respectively. The improvement rate in the TvL model decreases over time, whereas in the mean-field TLS model, it increases over time and finally converges to 1. It implies that the Pareto improvement is impossible for the TvL model, whereas it is possible for the mean-field TLS model. That is why we need to employ the interactions to the TvL model, and the interactive model is more persuasive. It is because the system that most people get poorer over time is untenable. In order to solve the equilibrium normalized capital distribution in the mean-field TLS model, we assume that $\langle C\rangle = C_0 e^{\tilde{\alpha}t}$. Figure S4 (b) shows the fact that $\alpha_{\rm ex}$ converges to $\alpha_{\rm ex}$. This value is related to the correlation between $\alpha$ and $c$ and slightly higher than $\alpha(\mu)\langle c\rangle \simeq \langle\alpha\rangle\langle c\rangle$. It means that the higher $\alpha$ guarantees the higher $c$ since their covariance is not zero even though it is small. The lower and upper bounds of $\tilde{\alpha}$ are $\alpha(r, g, b, T = 0)$ and $\alpha(r, g, b, T = 1)$, which correspond to the situations that all agents have the minimum effective talent and the maximum one, respectively. As shown in Fig. S4 (c) and (d), all $\tilde{\alpha}$ in mean-field models for a variety of talent distributions bounded with the following region: $\alpha(2, 0.1, 0.1, 0) = -0.0477 < \tilde{\alpha} < \alpha(2, 0.1, 0.1, 1) = 0.04805$. While the power-law exponent does not vary with the talent heterogeneity in the TvL model, see Fig. S2, it varies with the talent heterogeneity '$\sigma$' in the mean-field TLS model, see Fig. 3 (b) in the main text. As $\sigma$ increases, the power-law tail exponent $\gamma$ decreases. Consequently, in general, relatively richer agents occurs more frequent and the system inequality increases.

## S3. RANDOM PAIR SWAPPING ALGORITHMS

In order to control both $r_{\rm TA}$ and $r_{\rm TD}$ independently, we employ two algorithms as shown in Table S1 with schematic illustrations. Swap of node metadata to minimize (or maximize) the assortativity (similar with **Pseudo-code 1**) suggested by Cinelli *et al.* [15]. In our case, to estimate $r_{\rm TA}$ effect for a given network, we control $r_{\rm TD}$, and vice versa. However, $r_{\rm TA}$ and $r_{\rm TD}$ are correlated with each other under the single pair swapping. So we employ **Pseudo-code 2** in Table S1 to control the opposite talent configuration property. If $r_{\rm TA} = 0$, all agents are uncorrelated with regard to talent assortativity (TA), and vice versa. Therefore, we take the opposite value close to 0 as much as possible to minimize the opposite effect, We define such a zone as the 'quasi-pure zone' by taking $\epsilon = 10^{-2}$, so that these samples

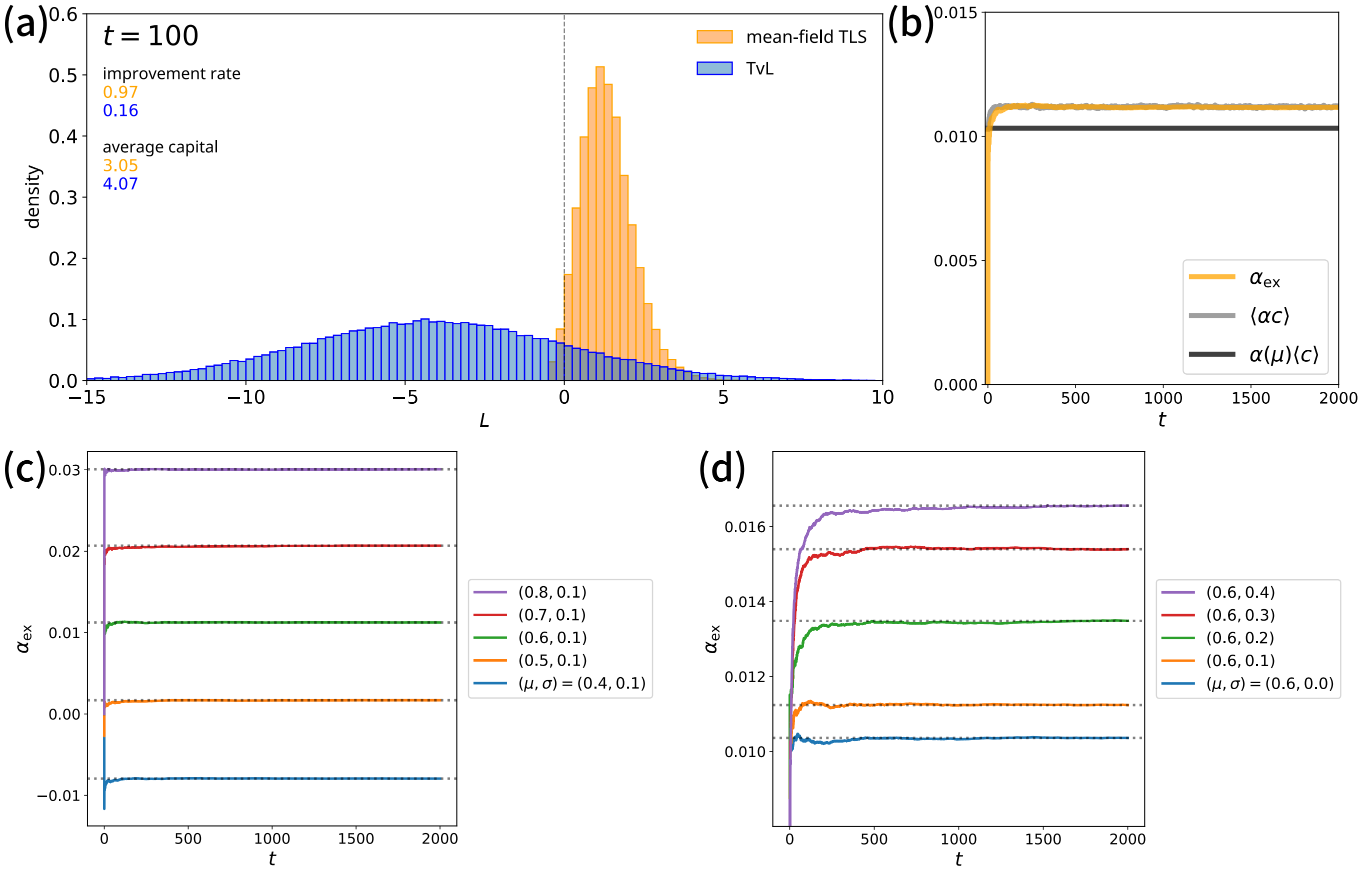


FIG. S4. Additional information for mean-field TLS model. (a) The $L$ distribution at $t = 100$ with $(\mu, \sigma) = (0.6, 0.1)$. While the improvement rate in the mean-field TLS model reaches about 1 at $t = 100$, in the TvL model, it is not. It means that when the Pareto improvement [23] is possible in the mean-field TLS model with enough time, whereas in the TvL, it is not. (b) $\alpha_{\mathrm{ex}}$ is related to the correlation between $\alpha$ and $c$ for $(\mu, \sigma) = (0.6, 0.1)$. (c) and (d) show how to converge $\alpha_{\mathrm{ex}}$ for a variety of parameters: (c) with the fixed standard deviation ($\sigma = 0.1$) and (d) with the fixed mean ($\mu = 0.6$).

are 'quasi-pure', $r_{\mathrm{TA}}$ and $r_{\mathrm{TD}}$, respectively.

## S4. MORE INFORMATION FOR TALENT CONFIGURATION EFFECT

### A. Quasi-pure samples of ($r_{\mathrm{TA}}$, $r_{\mathrm{TD}}$)

For Barabási-Albert (BA) and Watts-Strogatz (WS) networks [13, 14] with quasi-pure samples of $r_{\mathrm{TA}}$ and $r_{\mathrm{TD}}$ as shown in Fig. S5. Quasi-pure samples for BA and WS networks by using **Pseudo-code 2** in Table S1 with $N \times 100$ times of random pair swapping trials. Talent assortativity (TA, $r_{\mathrm{TA}}$) and talent-degree correlation (TD, $r_{\mathrm{TD}}$) are correlated under single pair swapping.

### B. All indices evolution over quasi-pure $r_{\mathrm{TA}}$ and $r_{\mathrm{TD}}$ for BA and WS networks

We show the time evolution of all three indices, where the simulation parameter sets are $(N, r, g, b, J, \mu, \sigma, \text{runs}) = (10^4, 2, 0.1, 0.1, 0.1, 0.6, 0.1, 2^{10})$. All lines are taken on the average indices of $2^{10}$ realizations. The upper dashed line is the average of the TvL model, the lower dashed line is the average of the mean-field TLS model, and the light-blue shadow portion indicates the intermediate region between them, see Fig. S6,S7.

Figure S6 shows the time evolutions of all three economic indices for BA and WS networks with the quasi-pure samples of $r_{\mathrm{TA}}$ ($r_{TD} \simeq 0$). The parameter set $(N, r, g, b, J, \mu, \sigma, \text{runs}) = (10^4, 2, 0.1, 0.1, 0.1, 0.6, 0.1, 2^{10})$ used. All lines are taken on the average indices of $2^{10}$ realizations. For $r_{\mathrm{TD}} \simeq 0$, $n_{\mathrm{rate}}$ cannot be larger than the case of the TvL

TABLE S1. Pseudo-codes for random pair swapping algorithms. In the left panel, a single value control (**Pseudo-code 1**, top) and dual value control (**Pseudo-code 2**, bottom) are shown, and in the right panel, four schematic illustrations are the processes of **Pseudo-code 1**.

**Pseudo-code 1 :** random pair swapping algorithm for $r_{\mathrm{TA}}(r_{\mathrm{TD}})$

**Data:** Graph $G$, talent vector $\mathbf{T} = (T_1, T_2, \cdots, T_N)$
**Result:** talent vector $\mathbf{T}'$

- **while** *Not* $|r_{\mathrm{TA}}(G, \mathbf{T}) - r'| < \epsilon$ **do**
  - $i, j \leftarrow \mathit{RandomInteger}[1, N]\ (i \leq j)$
  - $\mathbf{T} = (T_1, \cdots, T_i, \cdots, T_j, \cdots, T_N)$
  - $\tilde{\mathbf{T}} = (T_1, \cdots, T_j, \cdots, T_i, \cdots, T_N)$
  - **if** $|r_{\mathrm{TA}}(G, \tilde{\mathbf{T}}) - r'| < |r_{\mathrm{TA}}(G, \mathbf{T}) - r'|$ **then**
    - $\mathbf{T} \leftarrow \tilde{\mathbf{T}}$;
  - **else**
    - None;
- **return** $\mathbf{T}$;

**Pseudo-code 2 :** random pair swapping algorithm for **quasi-pure** $r_{\mathrm{TA}}(r_{\mathrm{TD}})$

**Data:** Graph $G$, talent vector $\mathbf{T} = (T_1, T_2, \cdots, T_N)$
**Result:** talent vector $\mathbf{T}'$

- **while** *Not* $|r_{\mathrm{TA}}(G, \mathbf{T}) - r'| < \epsilon_1$ *and* $|r_{\mathrm{TD}}(G, \mathbf{T})| < \epsilon_2$ **do**
  - $i, j \leftarrow \mathit{RandomInteger}[1, N]\ (i \leq j)$
  - $\mathbf{T} = (T_1, \cdots, T_i, \cdots, T_j, \cdots, T_N)$
  - $\tilde{\mathbf{T}} = (T_1, \cdots, T_j, \cdots, T_i, \cdots, T_N)$
  - **if** $|r_{\mathrm{TA}}(G, \tilde{\mathbf{T}}) - r'| < |r_{\mathrm{TA}}(G, \mathbf{T}) - r'|$ **then**
    - $\mathbf{T} \leftarrow \tilde{\mathbf{T}}$;
  - **else**
    - None;
- **return** $\mathbf{T}$;

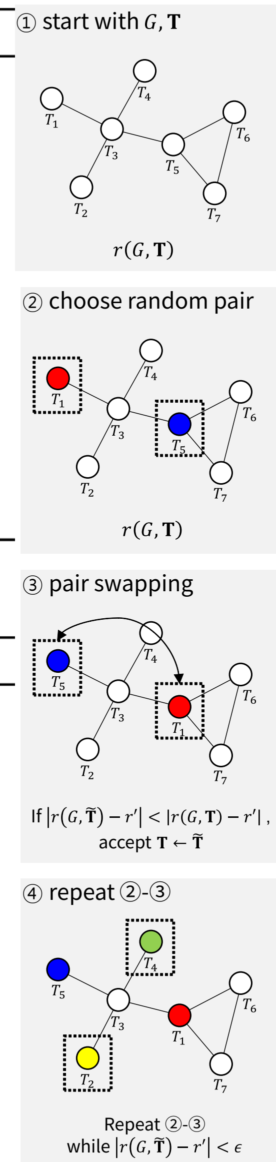


model, which is no matter how large $r_{\mathrm{TA}}$ value is. However, it can be smaller than case of the mean-field TLS model when $r_{\mathrm{TA}}$ is sufficiently small value. Thus, we suppose that $n_{\mathrm{rate}}$ of the TvL model is the upper bound of the TLS model without the talent-degree correlation effect ($r_{\mathrm{TD}} = 0$) as the corresponding detailed hypothesis.

Contrarily, for $r_{\mathrm{TA}} \simeq 0$, $n_{\mathrm{rate}}$ can be larger than the case of the TvL model when $r_{\mathrm{TD}}$ is sufficiently large. It shows that a choice and a concentration to highly talented agent give some advantage to the system with the aspect of capital growth in the short-term regime. For the BA network with the 'high-degree advantage', $n_{\mathrm{Gini}}$ almost lies in the intermediate range, only except in the short-term regime. The variances of $n_{\mathrm{Gini}}$ depend on $r_{\mathrm{TA}}$ more than $r_{\mathrm{TA}}$ for both cases. For $r_{\mathrm{TD}} \simeq 0$, $n_{LT}$ cannot be larger than 0, which means the pure effect of $r_{\mathrm{TA}}$ cannot make a tendency for less talented agents to become richer.

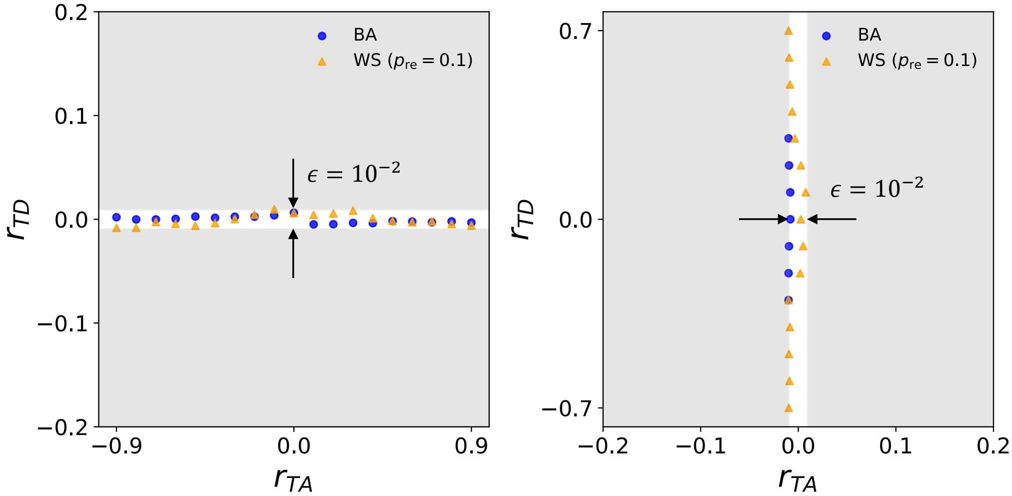


FIG. S5. Quasi-pure samples for BA and WS networks with $N \times 100$ times of random pair swapping trials.

## S5. TLS MODEL ON CYCLE NETWORK

We here discuss the role of talent configuration properties in the TLS model on the cycle networks. To do so, we first define the talent assortativity $r_{\mathrm{TA}}$ as follows:

$$r_{\mathrm{TA}} = \frac{Cov(T,T')}{\sqrt{Var(T)Var(T')}} = \frac{\sum_T \sum_{T'} TT'(e_{TT'} - q_T q_{T'})}{\sum_T T^2 q_T - (\sum_T T q_T)^2} = \frac{(1/M)\sum_i T_i T_i' - \left[(1/M)\sum_i \frac{T_i + T_i'}{2}\right]^2}{(1/M)\sum_i \frac{T_i^2 + T_i'^2}{2} - \left[(1/M)\sum_i \frac{T_i+T_i'}{2}\right]^2}, \tag{S2}$$

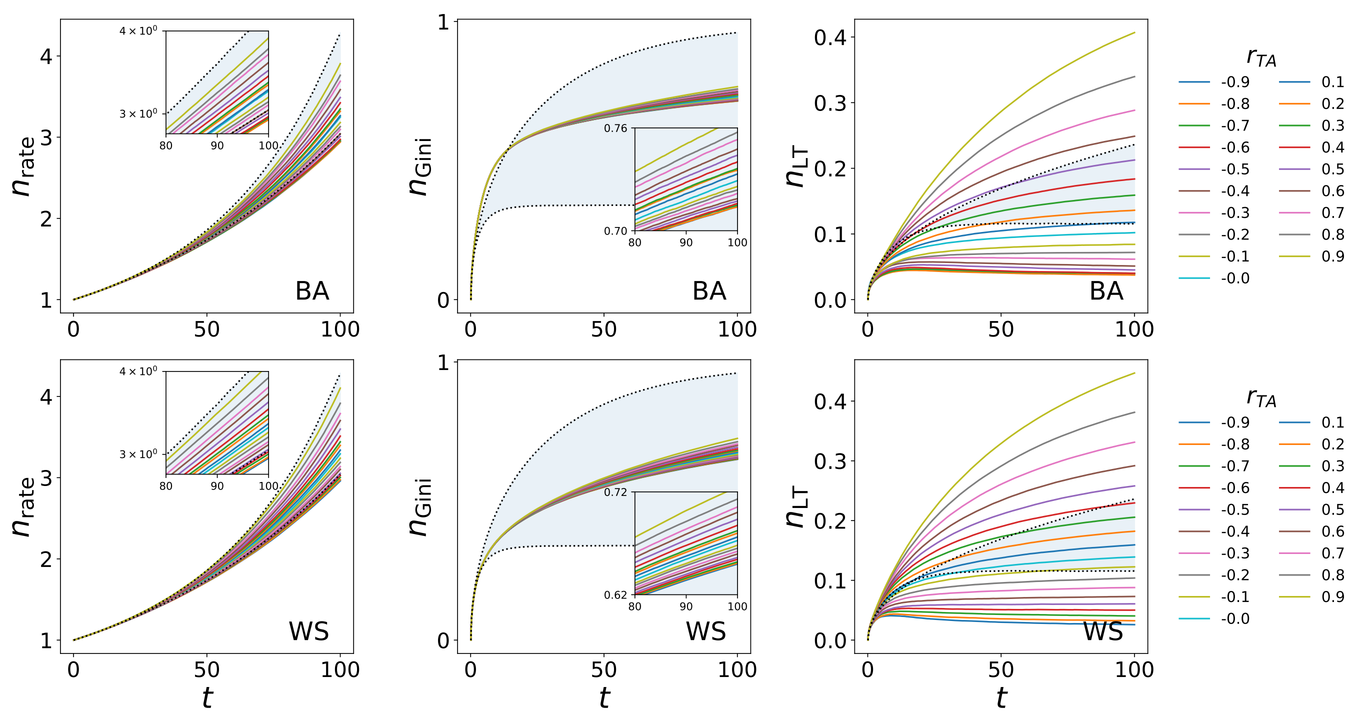


FIG. S6. TA effect on time evolutions of three economic indices in TLS model for BA and WS networks. The upper dashed line is the average of the TvL model, the lower dashed line is the average of the mean-field TLS model, and the light-blue shadow portion indicates the intermediate region between them.

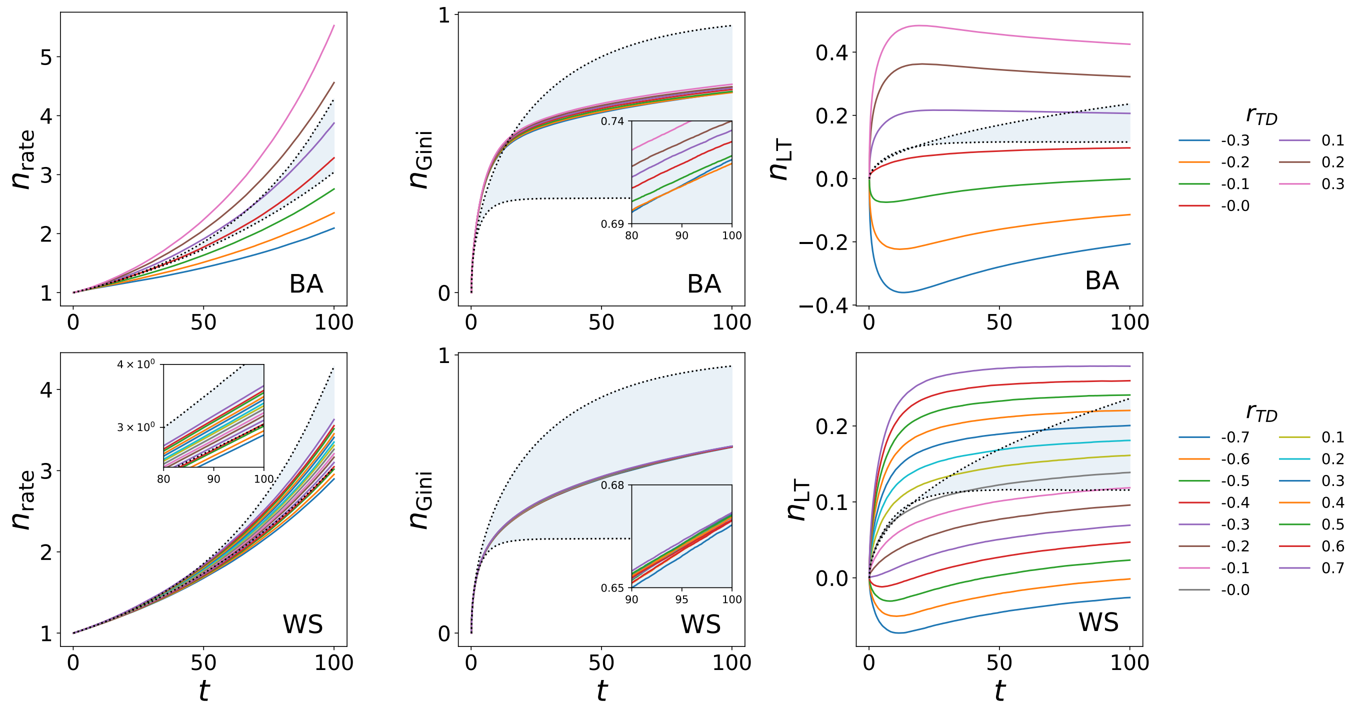


FIG. S7. TD effect on time evolutions of three economic indices in TLS model for BA and WS networks. The parameter set $(N, r, g, b, J, \mu, \sigma, \text{runs}) = (10^4, 2, 0.1, 0.1, 0.1, 0.6, 0.1, 2^{10})$ used. All lines are taken on the average indices of $2^{10}$ realizations. The upper dashed line is the average of the TvL model, the lower dashed line is the average of the mean-field TLS model, and the light-blue shadow portion indicates the intermediate region between them

The last one in Eq. (S2) is the empirical representation of $r_{\mathrm{TA}}$, where $i$ is a link index, $T_i$ and $T_i'$ are node talents for the selected link $i$, and $M$ is the total number of links.

The cycle network can have the minimum and maximum of $r_{\mathrm{TA}}$ as -1 and 1, which correspond to the minimum and maximum values of Pearson correlation coefficient. Consider the infinitely large ($N \to \infty$) cycle network. If $T$ follows the normal distribution for our case, random variable $T$ can be represented as $T = \mu + \sigma Z$ ($Z \sim \mathcal{N}(0, 1^2)$). If talent configuration is bisymmetric, connected node talents are almost all same that means $T' \sim T$. For the bisymmetric uneven case, $T' \sim \mu - (T - \mu)$. Lastly, for the random case, connected talents can be represented as serial chains, like $(x_1y_1 - x_2y_2 - \cdots - x_Ny_N)$ and $(y_1x_2 - y_2x_3 - \cdots - y_Nx_1)$. Here $x_i$ and $y_i$ are the samples of two independent normal random variable $X$ and $Y$. For that case, all connected talent combinations are uncorrelated if $X$ and $Y$ are uncorrelated.

$$\text{(bisymmetric uneven)}: \quad r_{\mathrm{TA}} \simeq \frac{\langle (T)(2\mu - T)\rangle - \langle T\rangle\langle 2\mu - T\rangle}{\sqrt{Var(T)Var(2\mu - T)}} = -\frac{\langle T^2\rangle - \langle T\rangle^2}{Var(T)} = -1, \tag{S3}$$

$$\text{(random)}: \quad r_{\mathrm{TA}} \simeq \frac{\langle XY\rangle - \langle X\rangle\langle Y\rangle}{\sqrt{Var(X)Var(Y)}} = \frac{\langle X\rangle\langle Y\rangle - \langle X\rangle\langle Y\rangle}{\sqrt{Var(X)Var(Y)}} = 0, \tag{S4}$$

$$\text{(bisymmetric)}: \quad r_{\mathrm{TA}} \simeq \frac{\langle TT\rangle - \langle T\rangle\langle T\rangle}{\sqrt{Var(T)Var(T)}} = \frac{\langle T^2\rangle - \langle T\rangle^2}{Var(T)} = 1. \tag{S5}$$

These results are consistent even if the talent distribution does not follow the normal distribution.

When $N \to \infty$, if talent configuration is bisymmetric, the connected subset of nodes can be regarded as the long chain of agents sharing the same talent. If the edge effect can be neglected, the subset system can be considered as an isolated node represented by a subset size. This subset have mean capital as

$$\langle C\rangle = C_0 e^{\alpha(T)t}$$

(as the result of the BM model) and exist at the ratio of $\frac{1}{\sigma\sqrt{2\pi}} e^{-(T-\mu)^2/(2\sigma^2)} dT$ in the entire ring. Thus, in that case,

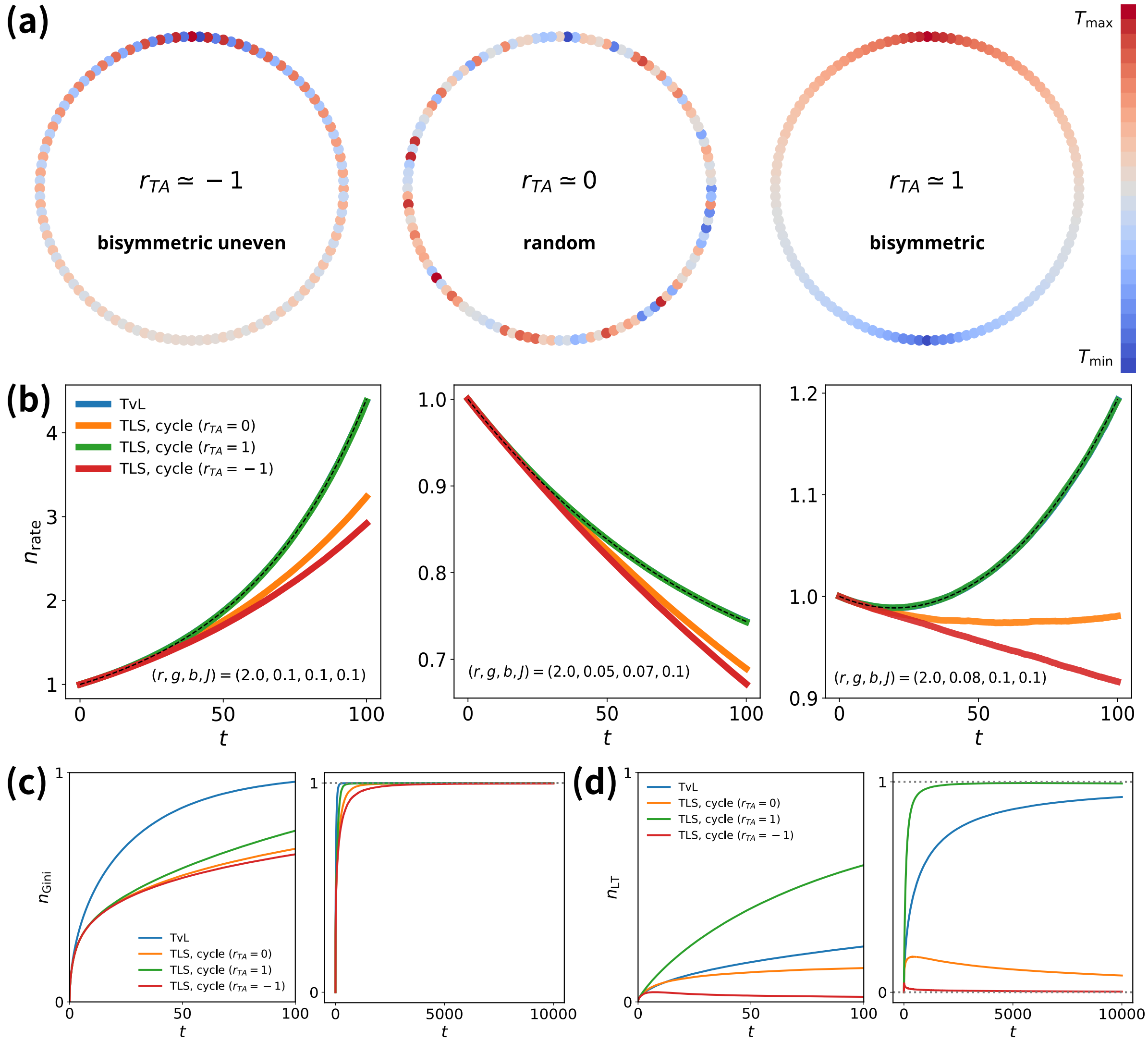


FIG. S8. The TLS model on a cycle network: (a) Three representative talent configurations for a cycle network. (b) The time evolution of $n_{\rm rate}$ in the TLS model on a cycle network for various conditions of $(g, b)$. $(r, \mu, \sigma) = (2, 0.6, 0.1)$ used. (c) The time evolution of $n_{\rm Gini}$. (d) The time evolution of $n_{LT}$. $(r, g, b, \mu, \sigma) = (2, 0.1, 0.1, 0.6, 0.1)$ used for (c) and (d).

the mean capital of the total system is

$$\langle C \rangle = \frac{1}{\sigma\sqrt{2\pi}} \int_{-\infty}^{\infty} e^{-(T-\mu)^2/(2\sigma^2)} C_0 e^{\alpha(T)t} dT,$$

exactly the same as the result of the TvL model. It is why the TLS model on the cycle network with $r_{\rm TA} = 1$ have the same value of $n_{\rm rate}$ as that of the TvL model even in the different conditions of $(g, b)$, see Fig. S4. (b).

One more interesting thing is that for the case of $r_{\rm TA} = 1$, $n_{LT}$ grows much more faster than the case of the TvL model. This is quite an interesting phenomenon because the interactions of the TLS model on regular network allow capital to be transferred from those with more capital to those with less. It is because more capital results in more talent on average in the long-term regime, and capital transfers are often from agents with more talent to agents with less talent. Therefore, in the presence of interaction, for most values of $r_{\rm TA}$, $n_{LT}$ is smaller than that of the TvL model (has no interaction) in the long-term regime. However, for $r_{\rm TA} = 1$, interaction leads to a perfectly meritocratic society much faster than the TvL model, see Fig. S8 (d). As mentioned in the main text, it can be considered as 'cartel effect'. On the other hand, for the case of $r_{\rm TA} = -1$, $n_{LT}$ converges to 0 after long-time that means there is any correlation between capital level $L$ and talent $T$. In other words, well-mixed talents on the network guarantee well-mixed capitals.